ANALYSIS AND PARTIAL DEVELOPMENT OF A SYSTEM FOR MEASUREMENT OF THE MOTIONS OF A SHIP MODEL IN SIX DEGREES OF FREEDOM

RICHARD O. HAUGHEY
AND
PETER J. DeLAAT, JR.

ANALYSIS AND PARTIAL DEVELOPMENT OF A SYSTEM FOR MEASUREMENT OF THE MOTIONS OF A SHIP MODEL IN SIX DEGREES OF FREEDOM

by

RICHARD O. HAUGHEY, LIEUTENANT, U.S. COAST GUARD

B.S., U.S. Coast Guard Academy

(1951)

and

PETER J. DELAAT, JR., LIEUTENANT, U.S. COAST GUARD

B.S., U.S. Coast Guard Academy

(1952)

SUBMITTED IN PARTIAL FULFILLMENT OF THE REQUIREMENTS

FOR THE DEGREES OF NAVAL ENGINEER AND MASTER OF SCIENCE

IN NAVAL ARCHITECTURE AND MARINE ENGINEERING

at the

MASSACHUSETTS INSTITUTE OF TECHNOLOGY

June, 1958

Signatures of Authors: _____

_____

Department of Naval Architecture and
Marine Engineering, May 26, 1958

Certified by: _____

Thesis Supervisor

Accepted by: _____

Chairman, Departmental Committee
on Graduate Students

ABSTRACT

ANALYSIS AND PARTIAL DEVELOPMENT OF A SYSTEM
FOR MEASUREMENT OF THE MOTIONS OF A SHIP
MODEL IN SIX DEGREES OF FREEDOM

by

Richard O. Haughey and Peter J. DeLaat, Jr.

Submitted to the Department of Naval Architecture and Marine Engineering on 26 May 1958 in partial fulfillment of the requirements for the degree of Naval Engineer and the degree of Master of Science in Naval Architecture and Marine Engineering.

The object of this investigation was to propose, analyse, and partially develop an angular and linear motion sensing system suitable for seaworthiness testing. It is anticipated that the principal use of the developed system will be in the measurement of model motions. In particular, ship model testing at the M.I.T. Towing Tank, and tanks of a similar character, was given full consideration.

Emphasis was placed on the selection of transducers, a proper mounting scheme to isolate undesirable disturbances and cross coupling effects between the inputs, and a suitable method to resolve the signals into independent components along the three chosen axes.

The feasibility of a system employing the use of three linear accelerometers and three rate gyros is believed to be established. The use of such a system affords a continuous time base record of linear accelerations, velocities, and displacements, as well as a record of angular rates and motions. In view of the characteristics of such a sensing package, it is felt that weight and space limitations of model carried equipment are no longer a problem.

The system, in its present state of development, will require additional study taking into consideration (a) refinement of the gravitational compensation system, and integrator balancing system, and (b) the laboratory mockup should include the use of rate gyros affording an accurate establishment of their performance characteristics.

Thesis Supervisor: Y. T. Li
Title: Associate Professor of Aeronautical Engineering

ACKNOWLEDGEMENTS

The authors wish to express their gratitude to the following who generously gave their time and assistance:

Professor Y. T. Li of the Department of Aeronautical Engineering, their thesis supervisor.

Professor M. A. Abkowitz of the Department of Naval Architecture and Marine Engineering, their thesis advisor.

Mr. J. Barley of the Department of Aeronautical Engineering Instrumentation Laboratory.

TABLE OF CONTENTS

LIST OF FIGURES

* Schematic Diagram

LIST OF TABLES

SYMBOLS USED

A	amplifier gain (amplification)
a	linear acceleration
C	capacitance in farads
c.g.	center of gravity
cps	cycles per second
E	electrical potential in volts
e	error
f	farads; also cycles per second
fps^2	feet per $(second)^2$ (linear acceleration)
g	gravity (32.165 fps^2)
i	current in amperes
j	square root of minus 1
K	one thousand
M	one million
N	revolutions per minute
R	resistance in ohms
s	distance
t	time in seconds
T	period (seconds/cycle)
V	volts
v	velocity in feet per $(second)^2$
x	longitudinal or surge axis
x	surge
y	transverse or sidle axis
y	sidle
z	vertical or heave axis
z	heave

α	angular acceleration (radians per second^2)
Δ	difference between
θ	yaw (rotation about the z axis)
μ	micro (10^{-6})
π	3.1416
τ	time constant (seconds/radian)
ϕ	roll (rotation about the x axis)
ψ	pitch (rotation about the y axis)
Ω	ohms
ω	angular frequency (radians per second)

Subscripts:

t	tangential
x	along the longitudinal axis
y	along the transverse axis
z	along the vertical axis
θ	yaw, or due to yaw
ϕ	roll, or due to roll
ψ	pitch, or due to pitch

I. INTRODUCTION

The problem to be treated in this investigation is the development of a system for accurately sensing the motions of a freely floated ship model. This definition implies one of the major constraints placed upon the system. That is to sense without inhibiting. The system will give full consideration to the character of the M.I.T. and similar towing tanks, placing emphasis upon their size and facilities available.

Recently there has been considerable interest, both analytical (43)* (25) and experimental (35) (39), in the problem of predicting the motions to be expected from a ship in rough seas, commonly termed seaworthiness evaluation. The most established means of accomplishing this goal is to make a study of model motions and then, by the use of Froude's Law of Geometric Similitude, to predict the desired ship motion.

There have been numerous systems developed for the purpose of measuring either specific motions (7) (40) or combined motions of a model (39) (36). These systems have employed the use of motion pictures, synchro transmitters, gyro transmitters, mechanically linked potentiometer pickoffs, and electromagnetic coupling. Stroboscopic (41) and flash-photography (42) methods have also been used. These systems suffer from one or more of the following disadvantages:

a. specific motion sensing devices are not adaptable to the uses of the present problem.

b. restraint of the model.

---

* Refer to Literature Citations, Appendix E.

c. excessive size and weight.

d. lack of a desirable level of precision.

e. the necessity of time consuming data reduction, which has the twofold effect of preventing rapid data analysis, and preventing the elimination of secondary effects that destroy the precision of the test results.

The system to be proposed uses a small sensing package, located at the center of gravity of the model, containing three linear accelerometers and three miniature rate gyros. Such a system will provide a continuous time base record of the three linear accelerations and their first and second integrals, as well as the three angular rates and their first integrals. There will be several major advantages to such a system. The overall weight of the sensing devices is a little less than a pound (this does not include a weight estimate of the mounting which they will require), and will occupy a volume approximately five inches by four inches, by four inches. The gyros mentioned in the earlier systems are of the free, or two gimbal, type and are not available in a miniaturized form. Consequently, their weight is of the order of six pounds (7), and the volume of a single unit is more than the entire package stated above. An inference may be drawn from the earlier portion of this paragraph that accelerations are considered more desirable than displacements. This is not consistent with the order of precedence established by the Thesis Advisor. However, it is felt that, by using the proposed system, it will be possible to obtain output signals of an accuracy somewhat superior to the presently available levels. (35) (39)

II. PROCEDURE

A. Establishment of the System Specifications

1. The system should be capable of measuring the displacements of the ship model in all six degrees of freedom.

2. The predicted range of accelerations and displacements to which the system will be subjected are tabulated on the following page in Table I.

3. The model carried components will not exceed five pounds maximum weight, and will not exceed the dimensions of four inches high, by four inches wide, by six to eight inches long.

4. The system will be made as accurate as possible, but the deviation should not in any case exceed 5 percent.

5. The system should be capable of adhering to these limits of accuracy for a period from two to four minutes with some consideration being given to a ten minute maximum.

6. It is intended that the overall system be capable of the measurement of both linear and angular quantities. In accordance with this intention, it was decided, after consultation with the Thesis Advisor, that the following precedence would be followed:

a. Precedence of signal resolution

   displacement

   velocity

   acceleration

b. Precedence of motion measurement

   roll

   pitch

   heave

TABLE I

System Specifications

Motion	Period (sec)		Amplitude		Acceleration		Velocity	
	Ship	Model	Ship	Model	Ship	Model	S	M
Heave	8-15	.8-1.5	10'-15'	.1'-.15'	$\sim$ 10 fps^2	$\sim$ 10 fps^2		
Surge	8-15	.8-1.5	15'-20'	.15'-.2'	$\sim$12.5fps^2	$\sim$12.5fps^2		
Sidle	8-15	.8-1.5	8'-10'	.08'-.1'	$\sim$ 6fps^2	$\sim$ 6fps^2		
Pitch	6-12	.6-1.2	7°-10°	7°-10°	.192rad/sec^2	1.92rad/sec^2	.183 rad/sec	1.83 rad/sec
Roll	12-18	1.2-1.8	Up to 60°	Up to 60°	.288rad/sec^2	2.88rad/sec^2	.55 rad/sec	5.5 rad/sec
Yaw	8-15	.8-1.5	$\sim$ 5°	$\sim$ 5°	.054rad/sec^2	.54rad/sec^2	.0686rad/sec	.686rad/sec

NOTES:

(1) z and ψ are from (35)

(2) Surge is based on a full scale speed oscillation from 0 to 5 knots

(3) Angle of Roll is from chapter 8, page 49 of (34)

(4) Periods of z, x, y, and θ are periods of wave encounter (2)

(5) Scale factor = 100

surge

sidle

yaw

B. Factors Considered in the Selection of Relative Motion Receivers (1)

1. Type of Input.

   linear

   angular

2. Input range.

3. Maximum uncertainty in the low input magnitude range.

4. Maximum uncertainty in the high input magnitude range.

5. Dynamic characteristics.

6. Availability.

7. Size and shape of space occupied.

8. Weight.

9. Useful life and reliability.

10. Maintenance.

11. Cost.

C. Factors Considered in Relation to the Over-all System Performance (1)

1. Sensitivity to electrical interference.

2. Services required for operation.

3. Ease of operation.

4. Size and weight of complete system.

5. Reliability.

6. Cost.

D. Possible Types of Sensing Elements Considered

1. Linear accelerometers.

2. Angular accelerometers.

3. Rate gyros.

4. Integrating gyros.

5. Free gyros.

E. Possible Combinations of Sensing Elements to Measure Displacements in Six Degrees of Freedom

1. Six linear accelerometers.

2. Three linear accelerometers and three integrating gryos.

3. Three linear accelerometers and three rate gyros.

4. Three linear accelerometers and two free gyros.

5. One linear accelerometer capable of sensing the three mutually perpendicular linear accelerations, and two free gyros.

6. Three linear accelerometers and three angular accelerometers.

7. Six gyros with adjoining masses on beams.

8. Three linear accelerometers capable of simultaneously sensing linear accelerations along two mutually perpendicular axes.

F. A General Discussion of Some Factors Relating to the System Design and the Selection of Sensing Elements

The proposed sensing system is to be mounted on an unstable platform, which will be simultaneously rotating and translating. This mode of excitation is to the best of the authors' knowledge a new application for the proposed linear accelerometers.

It was established, after consultation with the Thesis Advisor, that the system should sense motions with respect to a coordinate system which is fixed with respect to the ship model, as opposed to an inertial coordinate system. This is a rather obvious conclusion, since it is only those motions along ship axes which are consistent with the stated objectives of the thesis. The thought may occur here, however, that it would have been considerably simpler to consider an

inertial coordinate system, and to make use of motion sensing systems of a similar character already known to exist in the pilotless aircraft, missile, or rocket fields. This is an accurate, but somewhat specious thought. The existing systems are quite bulky (22), in relation to the stated specifications of the desired system, and would require a coordinate transformation. This latter requirement would have several disadvantages. (a) It would be complex. (b) If this coordinate transformation were feasible electronically it would probably be both expensive and, within the details of its own design, quite complex. (c) If it were not feasible electronically it would require an amount of data reduction, which would be a serious disadvantage in relation to existing model sensing systems. In this same vein it may be mentioned that the accelerometer package of an inertial guidance system, whether of the pendulous or single axis linear accelerometer type, is unsuited to the use of this design. There are a number of reasons for this. Some of the more obvious are (a) it is mounted on what amounts to a stable platform (23), and consequently suffers from the coordinate transformation difficulties mentioned above, and (b) in the process of arriving at the stable platform it makes use of integrating gyros, which are themselves undesirable pieces of equipment, as will be demonstrated below.

In accordance with the intentions of the Preliminary Report dated 22 January 1958 which states "---the first portion of the thesis will be devoted to the study, and analysis of various systems. Upon completion of this portion, a single system will be selected for further development. If the components of the selected system are available the thesis will proceed with the construction, calibration, and testing of this system. If the components are not available an evaluation of

the possibility of the construction of the desired components will be made,---" section "E" of this procedure was prepared with the specific intention of not limiting consideration of the possible combinations of transducers to known and available commercial models. An effort was made rather to consider the physical characteristics of the desired sensing system in light of the stated specifications, and while generally channeling the creative thought to those first principles utilized by successful transducing devices, an attempt was made to propose an instrument which might be better suited to the particular design problem under consideration. Reference is being made here, in particular, to linear accelerometers.

It may be stated at this point that the same device which is used for the measurement of linear accelerations may also be used for the direct measurement of displacements (a seismograph), provided the natural frequency of the instrument is properly chosen. In light of this fact, the question might be very reasonably asked, if it has not occurred already, "Why were not displacement meters, rather than linear accelerometers, chosen as transducers in accordance with the precedence of signal resolution specified on page 3?" The answer lies in the fact that it is considerably easier (though by no means a small task) to double integrate than it is to accurately carry out a process of double differentiation (5). A somewhat contrasting, but nevertheless consistent opinion concerning the choice of linear accelerometers is contained in the following quotation; (23)
"A satisfactory electrical integrator or differentiator within the optimum frequency of a vibrometer or accelerometer is relatively easy to obtain. For this reason an evaluation of the relative merit of an accelerometer system against a vibrometer system can be made, based

upon the property of the pickup alone. Generally speaking, an accelerometer is more desirable than a vibrometer. Firstly, for low frequency application of less than 5 cps, there are few satisfactory vibrometers available. Anything below 1 cps is almost nonexistent. ——— The construction of an accelerometer tends to be much smaller than a vibrometer. This is especially true if a large amplitude of vibration is to be measured. Because no suspension problem is involved, an accelerometer tends to be simpler and should therefore be less expensive. For this reason, the vibrometer as an instrument has little future, although there still seems to be a market for it."

One more question of a general nature which may be asked at this time is, "Doesn't the vessel in fact roll about the virtual center of gravity (24) instead of the actual center of gravity, and since the linear accelerometers must be placed at this center of gravity in order to reduce the somewhat considerable errors (developed below) due to angular motions, the system might well prove to be impractical?" Here again it is rather easy to confuse the elements of this design problem with those of existing analyses. The concept of the virtual center of gravity results from a consideration of the virtual mass of a body used for the determination of the inertia forces experienced by a model in a perfect fluid. These inertia forces are then used for the analytical prediction of the motions of a ship. (25) The concept of added mass together with that of the virtual center of gravity is then seen to be an analytical concept employed for the successful prediction of ship motions. The proposed sensing system is not concerned with the prediction of, but the measurement of the model motions, and consequently need not concern itself with the concept of the virtual center of gravity or its movements.

G. Specific Analysis of the Possible Types of Sensing Elements Considered

The analysis contained below is somewhat abridged from its original form. It is felt that it would be redundant to repeat in the case of each instrument the numerous factors mentioned under paragraphs "B" and "C" above. Rather, reference will be made to the particular manufacturer's catalogue from which the desired information may be obtained. In other words, the intention is to present those elements of the analysis which are more closely related to the particular design under consideration and, by so doing, to prevent occlusion of some of its more salient features by an unnecessary amount of detail.

1. Linear Accelerometers:

(a) Linear accelerometers, regardless of type, are essentially simple, seismic, second order, single-degree-of-freedom systems. Table II (19) lists some of the more prevalent types and presents their general characteristics.

(b) The signal from the linear accelerometers will require double integration before displacements are obtained.

(c) It was originally proposed to use sum and difference operations on the output of the two linear accelerometers in the manner presented in Figure I, with the instruments displaced from one another along a ship's axis. Figure II* demonstrates that at the maximum displacement allowed by the proposed system specifications (two inches either side of the system center of gravity), the tangential acceleration due to the largest predicted angular acceleration (roll) is only .96 fps^2. The order of magnitude of this signal may be contrasted visually with those of the predicted linear signals (surge,

---

* For sample calculations see Appendix D.

TABLE II

Various Types of Linear Accelerometers (19)

Type of Accelerometer	Acceleration* Range in g's	Frequency* Range	Accessories Required	Accuracy ±**	Temperature Range °F
Piezoelectric	0.001-20,000	3-20,000	Cathode follower required for measurements below 200 cps.	5	-65 to + 500
Strain Gauge	0.01-1,000	dc-1,500	Carrier excitation (ac or dc) balance circuit.	1	-65 to + 250
Vibrating Wire	-	dc-20,000	Special amplifier and oscillator.	2	Temp. controlled at 130°
Variable Reluctance	0.1-75	dc-300	Carrier excitation.	3	-65 to + 165
Electronic	0.01-75	dc-300	Stable power supply and zeroing control.	2	-65 to + 250
Differential Transformer	0.01-1,000	dc-500	Carrier excitation, balance circuit, demodulator.	1	-65 to + 165
Potentiometer	0.2-75	dc-60	Excitation (ac or dc).	2	-65 to + 165

* These ranges are not for one instrument, but for several in each category.

** Accuracy ± Including Linearity Hysteresis, Repeat in Percentages

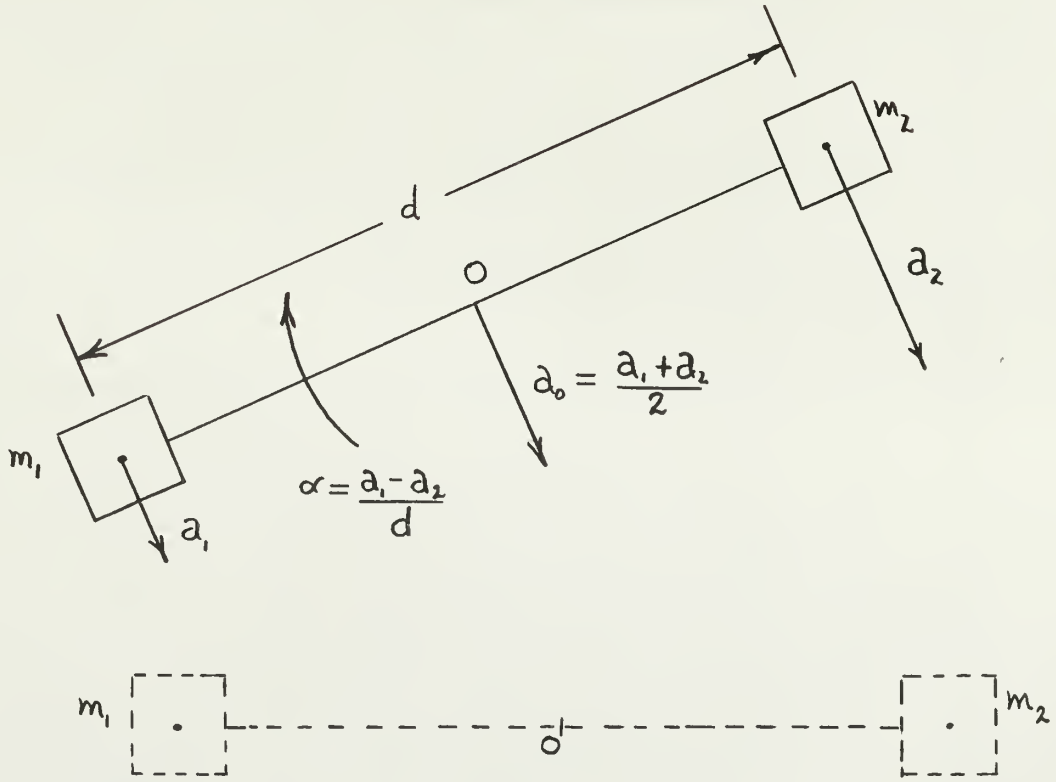

FIGURE 1

Measurement of Both Linear and Angular Periodic Accelerations With Linear Accelerometers

FIGURE II

Feasibility of Using Linear Accelerometers
To Sense Angular Motion

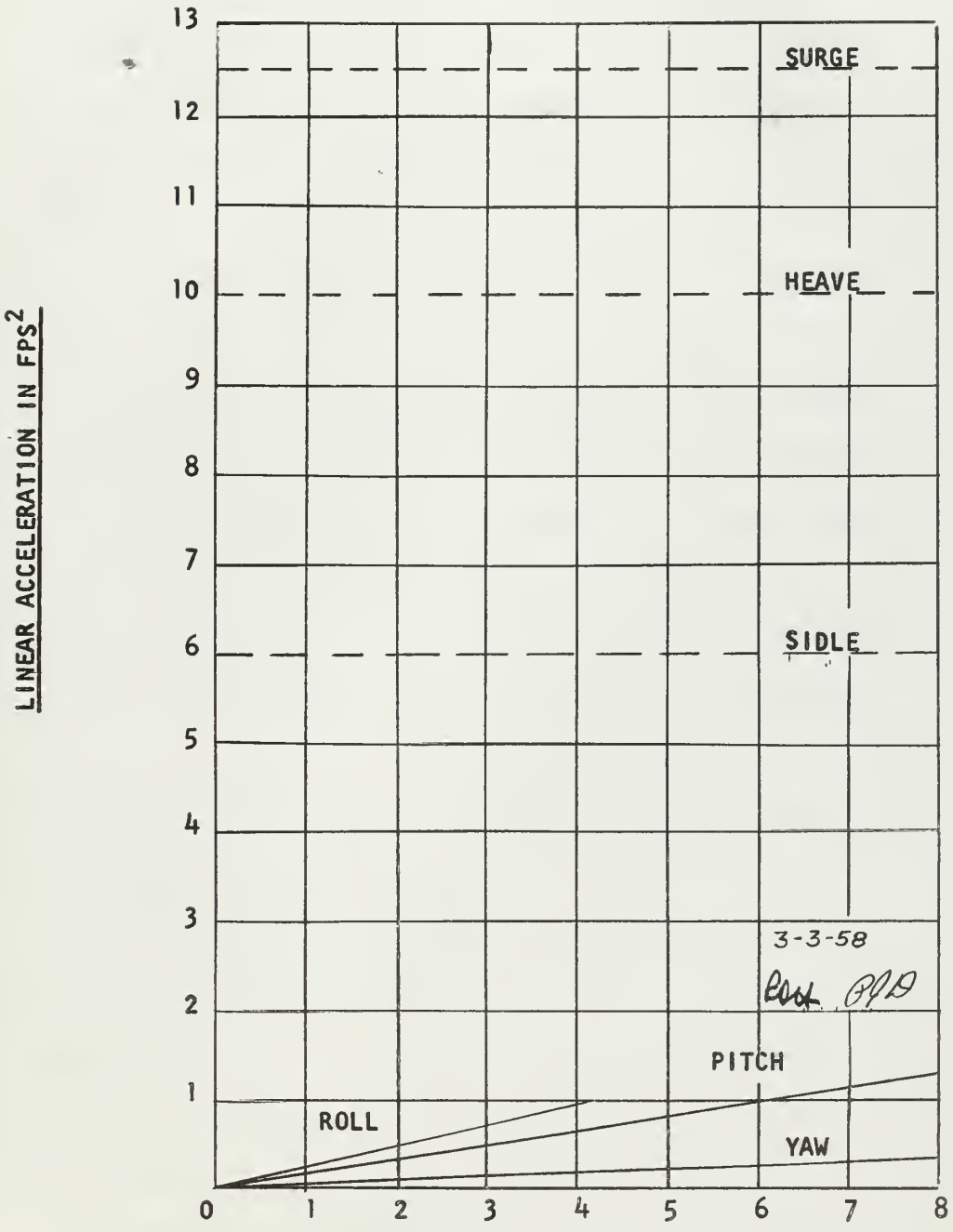

heave, and sidle). It was felt that such a low level signal might well be obscured by errors due to non-linearity alone, and in view of the motion measurement precedence, previously established, the use of six linear accelerometers as possible angular sensing devices was effectively ruled out.

(d) At this point in the procedure it becomes clear that the sensing of angular accelerations by the linear accelerometers, either normal or tangential, is an undesirable occurrence. An ideal design for the purpose of reducing angular acceleration effects would be one linear accelerometer capable of sensing the three mutually perpendicular linear accelerations, to be placed at the center of gravity of the model. Consistent with the general intentions of the thesis, some thought was given to the design of such a device. This avenue of investigation was concluded with the observation that since existing accelerometers cannot be designed to within a closer tolerance than 0.02 g per g for response to transverse accelerations, a continued pursuit of this study would probably produce an instrument whose characteristic in this respect is somewhat in excess of the above, and consequently unsuitable for the purposes of the proposed system.

2. Angular Accelerometers:

Angular accelerometers possess response specifications (11) suited to the requirements of the proposed system. However, they are unsatisfactory from the point of view of weight and space, and consequently were not selected for further consideration.

3. Rate Gyros, Integrating Gyros, and Free Gyros:

In contrast to the individual treatment of the linear and angular accelerometers, it is felt that there is little to be gained from such a breakdown of the analysis of the various types of gyros.

While there are a number of considerations to be applied in the selection of the type of gyro to be used for the measurement of a particular input, the choice was limited in this case by the size specifications of the transducer package. The result was the selection of the miniature rate gyro. (8), (9), (10). An evaluation of the errors anticipated from the use of this instrument is included in the Discussion of Results.

H. Analysis of Linear Accelerometer Errors Due to Rotational Motions of the Model

In view of the character of the acceleration sensing devices, it is apparent that any displacement of their sensitive masses from the center of gravity of the model will result in an output signal due to the algebraic sum of those components of normal and tangential accelerations coincident with their sensitive axes. At this point in the procedure it was realized that the most direct optimization process for minimizing the errors resulting from this effect would be to develop three sets of curves per axis for various positions of an accelerometer along any given axes. These curves are plotted on Figure XII. Sample calculations for these curves are shown in Appendix D.

I. Choice of the Specific Linear Accelerometer Models and Their Proposed Positional Arrangement

In response to correspondence with the Statham Laboratories, specifications (3) and data (12) were obtained for the purpose of selecting particular accelerometer models. Heavy paper mockups of the various models were constructed, facilitating a realistic determination of the accelerometer package size. Numerous configurations of the models were tried in order to arrive at an optimum arrangement. This procedure considered, in addition to those factors mentioned above,

(a) Figure XII, (b) the precedence of motion measurement, and (c) a desirable damping coefficient. In view of the system specifications and (12) there is good reason to believe that a damping coefficient of something less than .7 would be desirable. However, this nominal value was adhered to with the intention of not limiting the usefulness, or number of possible applications, of the proposed instruments. The selected instruments and their configuration are shown in Figure XIII.

J. Choice of the Specific Rate Gyro

The selection of satisfactory rate gyro models has been mentioned on page 15. This paragraph is entered primarily for the purpose of continuity and to mention that it was determined, after their selection, that the rate gyros could not be delivered within a period of time that would be satisfactory for the Thesis.

K. Static Calibration of the Linear Accelerometers

The accelerometers were simultaneously calibrated and examined for linearity and hysteresis effects by the simple procedure of rotating them, at fixed intervals, through 360 degrees in the earth's gravitational field. Tabulated data for these tests is contained in Appendix C. The results are shown on Figures XIV through XIX.

The calibrating setup was composed of equipment listed in Appendix E. Prior to commencement of calibration, the longitudinal axis of the Hardinge dividing head was aligned horizontally by the use of precision levels. Then the accelerometer models were placed in a 4 jaw chuck on the dividing head and their cases aligned with the long dimension of the instrument vertical, and the short dimension brought into the horizontal plane by means of adjusting and zero setting the calibrated face of the dividing head. With the instruments thus aligned, they were provided with battery excitation and their output

recorded at the various angles of inclination by means of a precision potentiometer, in conjunction with an auxiliary, or external galvanometer. (38)

L. Consideration of the Instruments Response to Transverse Accelerations

The manufacturer's specifications (3) for these instruments states that they have a response to the vector sum of those accelerations in a plane normal to their sensitive axis of .02 g per g. Figure XX was prepared with the intention of evaluating the predicted variation of this error and is believed to be self explanatory.

M. Gravitational Error Analysis

This analysis was somewhat lengthy and consisted of graphical presentations of a number of somewhat complex expressions for the purpose of arriving at a simple but satisfactory expression which might lend itself to electronic reproduction. The procedure followed here was to (a) develop curves defining the actual variation of the gravitational error present during the various motion measurements, (b) consider approximation of the error by making use of a Taylor's series expansion, and (c) consider approximation of the error by the use of trigonometric functions. Results of this procedure are shown on Figures XXI through XXIV. Derivation of equations used is contained in Appendix B, and a summary of calculations in Appendix C.

N. The Proposed Sensing System

The proposed system, Figure XXVIII, was based on all of the foregoing procedure in addition to the following considerations:

(a) signal attenuation due to integration.*

(b) trigonometric function generation by means of the

---

* See Appendix D.

"Sine-Cosine Operator." (26)

(c) trigonometric function generation by means of servo driven sine-cosine potentiometers. (21), (27), (31), and (32)

(d) characteristics of, and type of recording system. (33)

O. Laboratory Procedure

After completing the proposal of the desired sensing system, an effort was made to ascertain its feasibility by submitting a number of its components to laboratory test.

Prior to the commencement of the tests, however, it was necessary to assemble the Double Integrating Summing Amplifier shown pictorially in Figure III, along with a suitable calibrating platform shown pictorially in Figure IV. The Double Integrating Summing Amplifier made use of two Model USA-3, Philbrick operational amplifiers. (20) A schematic presentation of a single stage is shown in Figure V, and a derivation of its theoretical frequency response is included in Appendix B. The calibrating table is a relatively simple device which allows the accelerometer to be subjected, simultaneously, to a static gravitational acceleration, at various angles of inclination, while experiencing dynamic accelerations consistent with the predicted amplitudes stated in the system specifications.

The tests which were carried out are as follows:

1. Calibration of the Sine-Cosine Potentiometer.

The procedure employed for the static calibration of the sine-cosine potentiometer was quite similar to that employed for the static calibration of the linear accelerometers. The equipment used is listed in Appendix E, a sample calculation for the voltage divider circuit is included in Appendix D, and a schematic diagram is included in Figure VI. The shaft of the potentiometer was secured in the jaws of the dividing

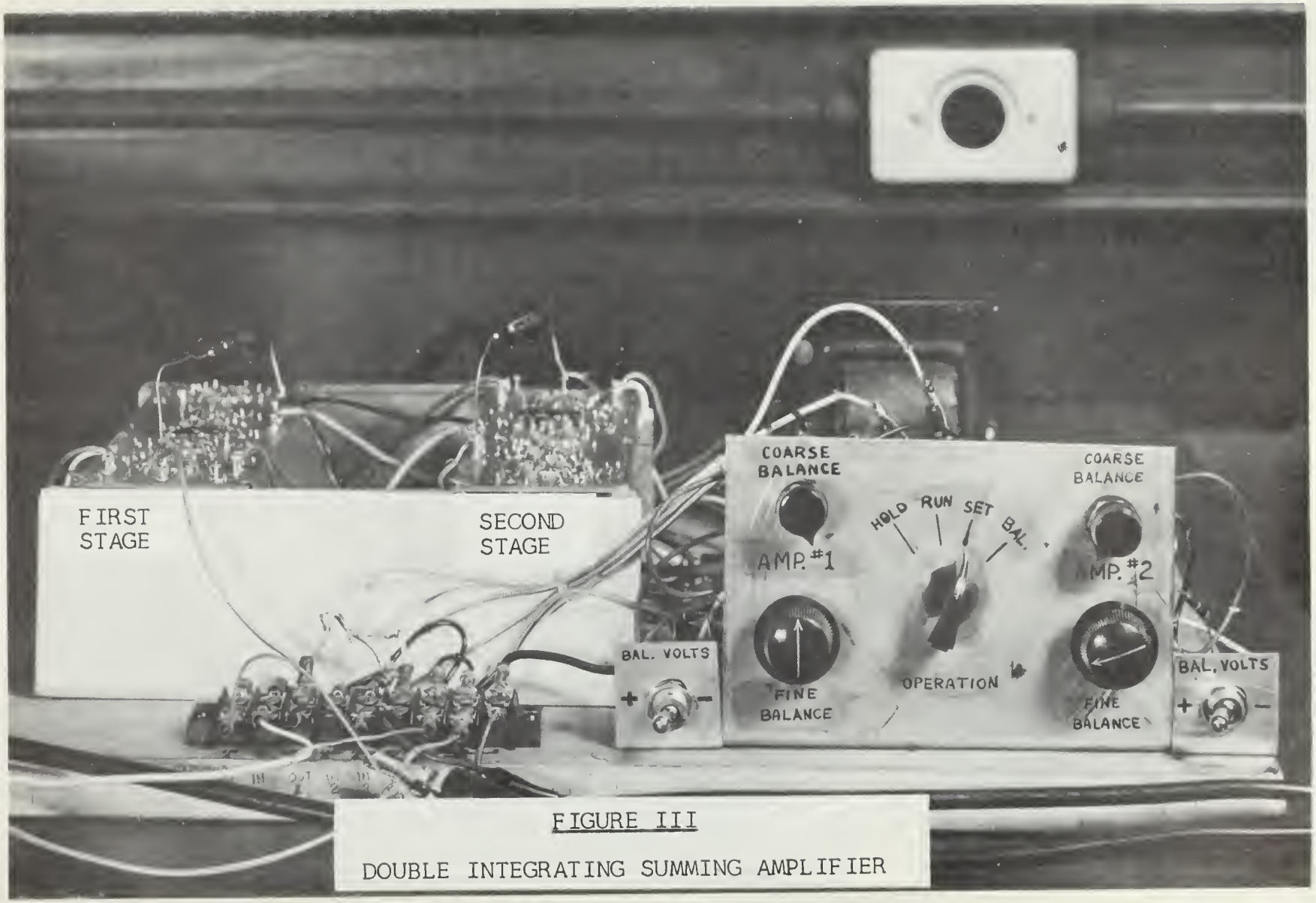

FIGURE III

DOUBLE INTEGRATING SUMMING AMPLIFIER

FIGURE IV

CALIBRATING TABLE

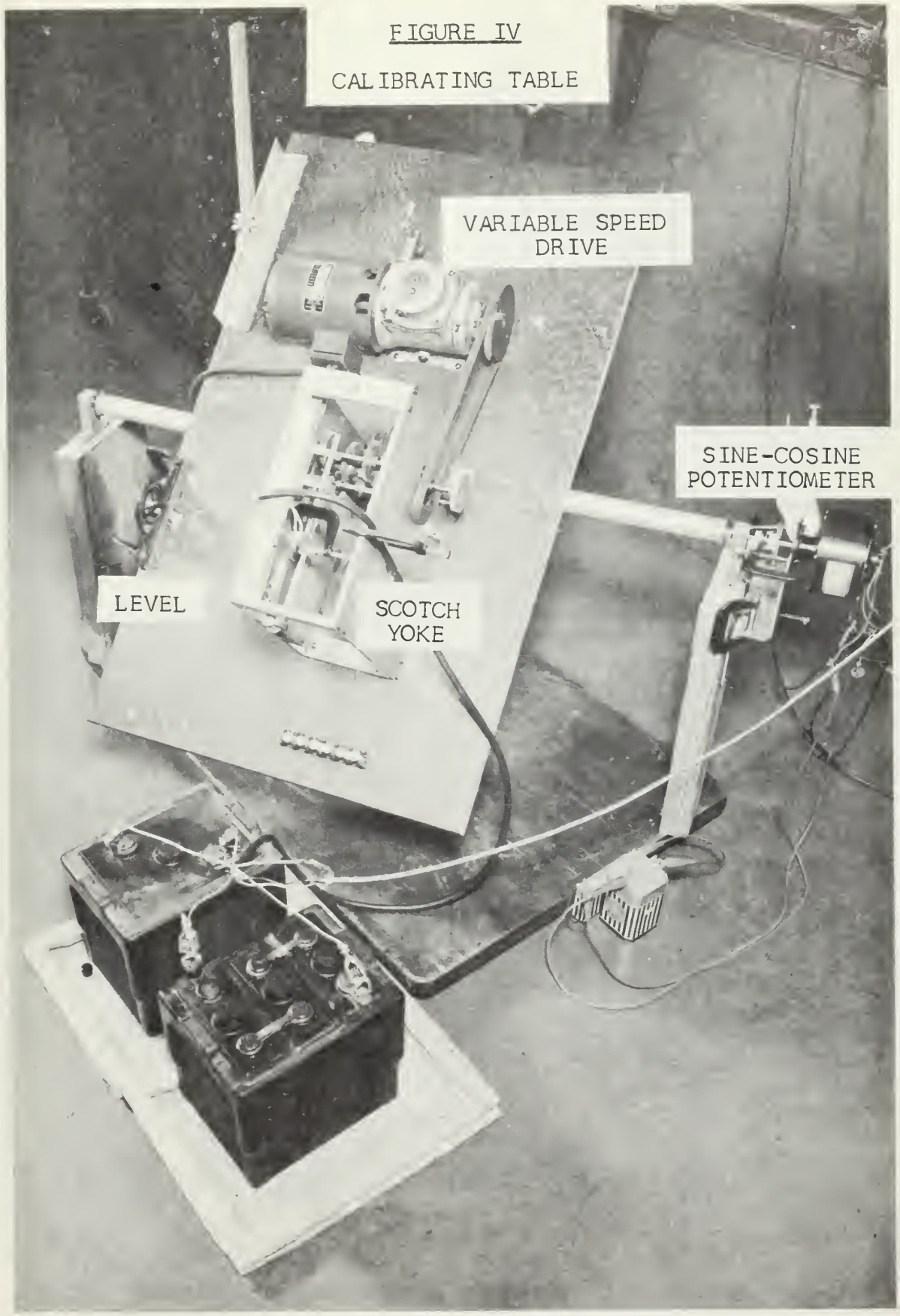

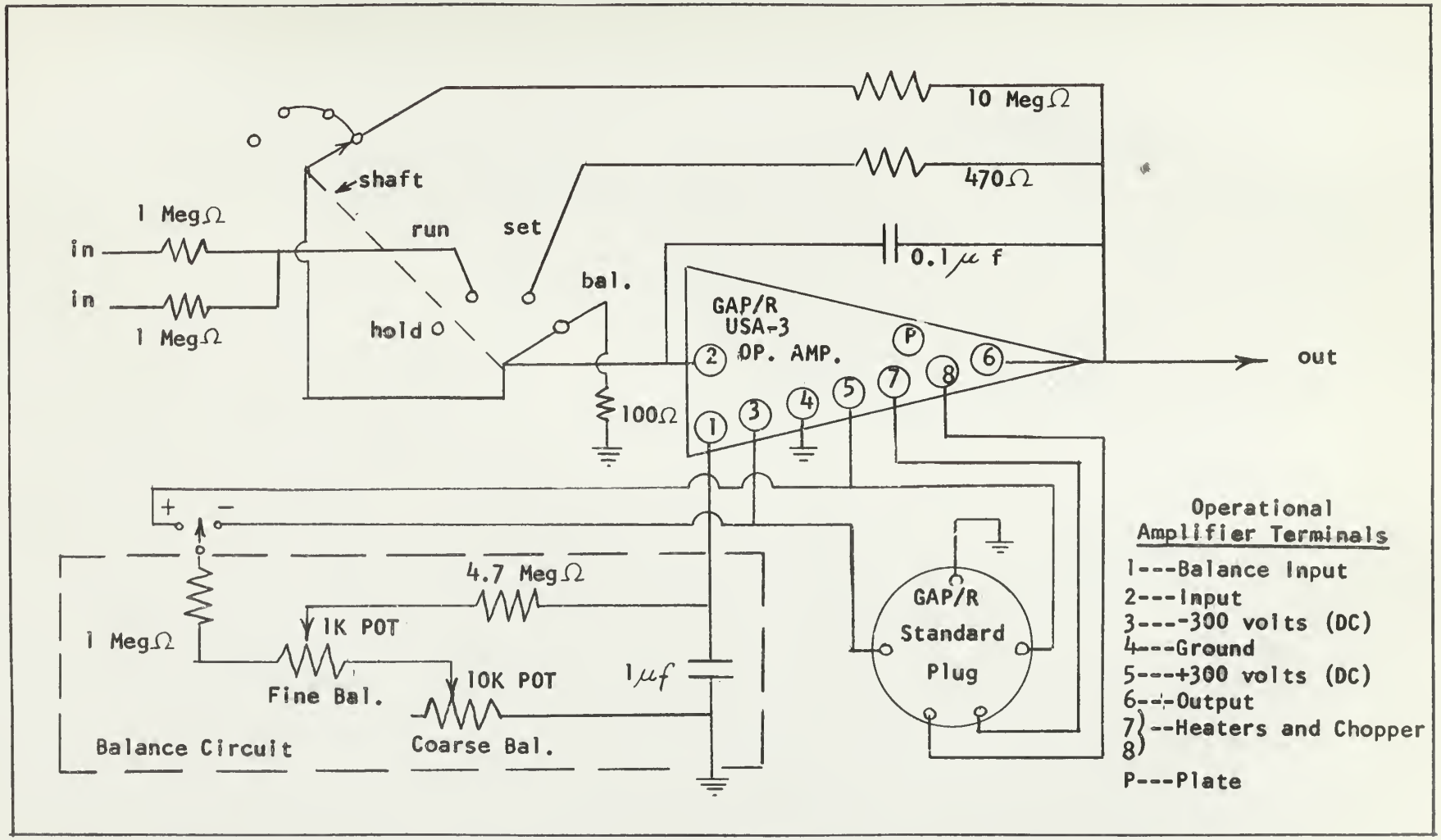

FIGURE V

Integrating Amplifier

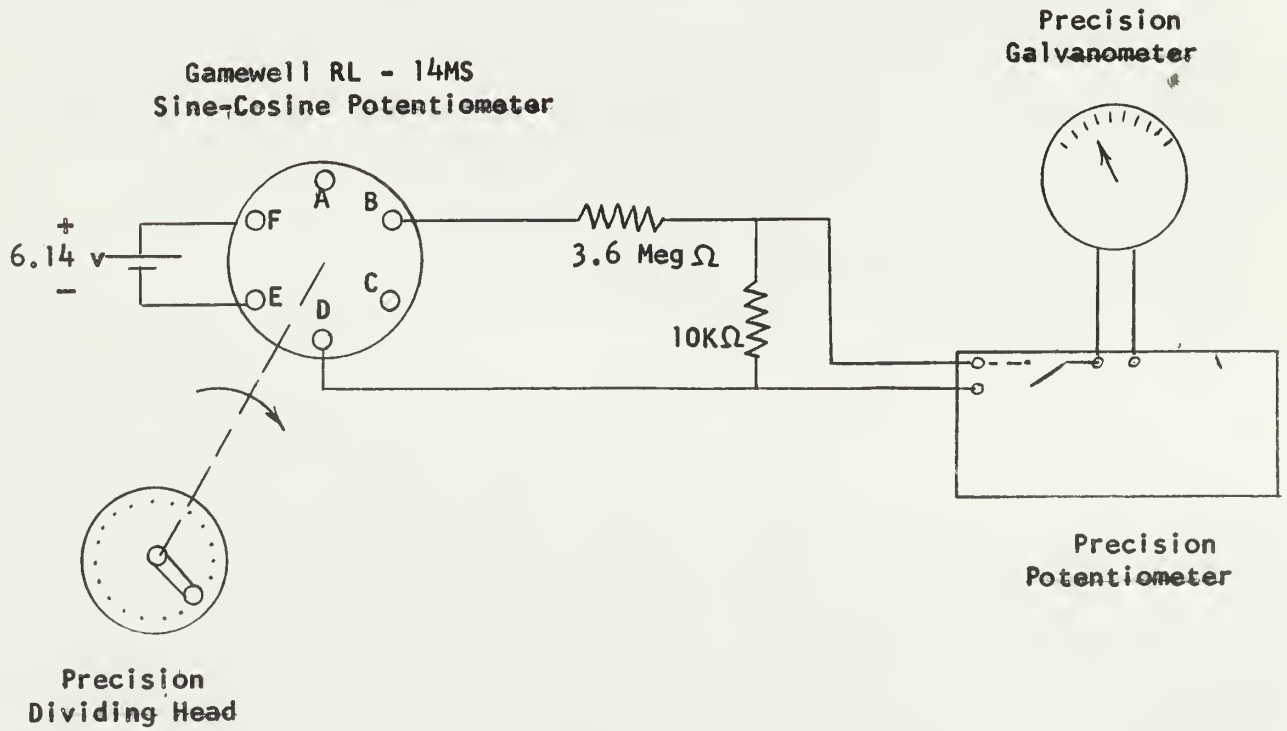

FIGURE VI

Sine-Cosine Potentiometer Calibration

head while taking care to support the potentiometer housing in such a manner as to prevent wobbling of the shaft while rotating it through 360 degrees.

2. Ability of the Sine-Cosine Potentiometer to Null Gravitational Errors.

With the accelerometer and potentiometer mounted as shown in Figure IV, the output signals of the two instruments were recorded in Table XI , and compared graphically in Figure XXX.

The essential steps carried out during this test are (a) the outputs of the two instruments were established at zero with the table horizontal, (b) the table was rotated to an angle of forty-five degrees, and the accelerometer output was measured, (c) by varying the decade resistor, shown in the schematic diagram Figure VII, the magnitude of the voltage divider pickoff was made the same as that of the accelerometer output, and (d) with the system thus adjusted the table was rotated back into the horizontal, in five degree steps, while recording the output of the two instruments.

3. Double Integrator Response to a Constant Displacement Input.

Prior to the commencement of this test, the output of the accelerometer was established at zero with the table horizontal. A schematic diagram of the circuit components and their connection is shown in Figure VIII. A picture of the components is shown in Figure IX, and an equipment list is included in Appendix E.

The full travel of the Scotch Yoke, Figure X, was measured with a steel rule and found to be 4.763 inches. The initial speed of the yoke was determined to be 76 rpm by use of a stop watch.

With the equipment set up as described above, the rpm of the Scotch Yoke was varied over the frequency range shown in Figure XXXI.

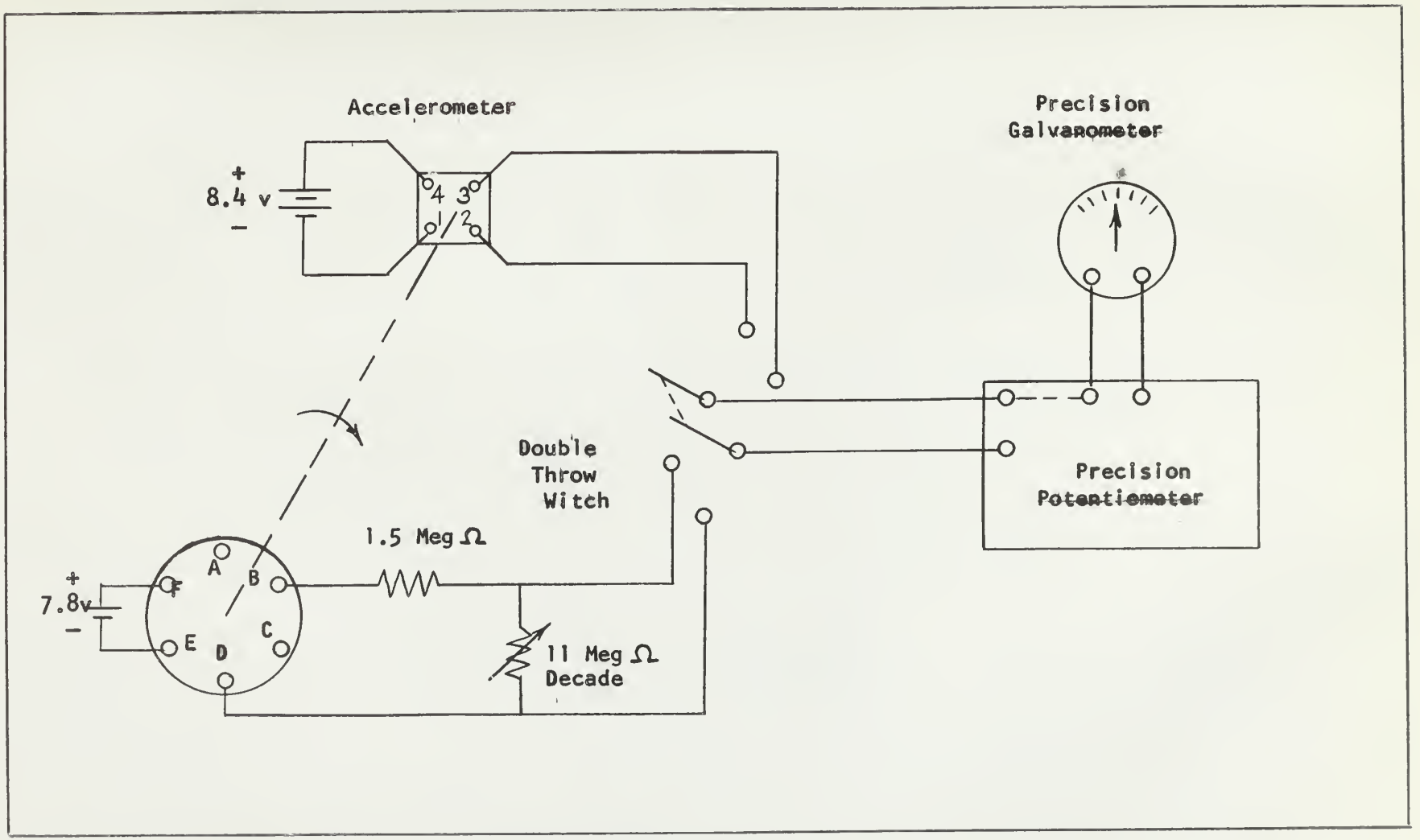

FIGURE VII

Ability of the Sine-Cosine Potentiometer to Null Gravitational Errors

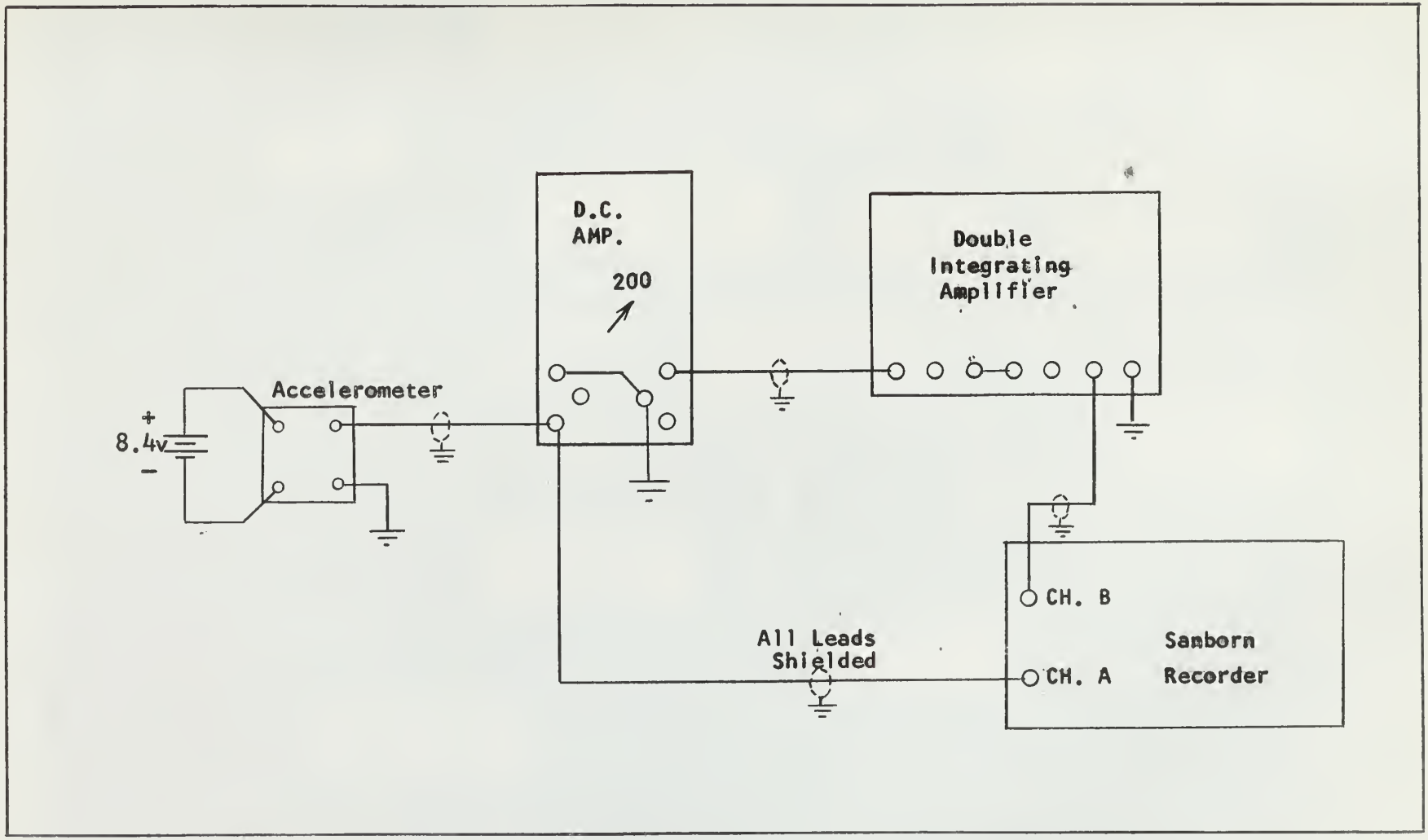

FIGURE VIII

Double Integrator Response to a Constant Displacement Input

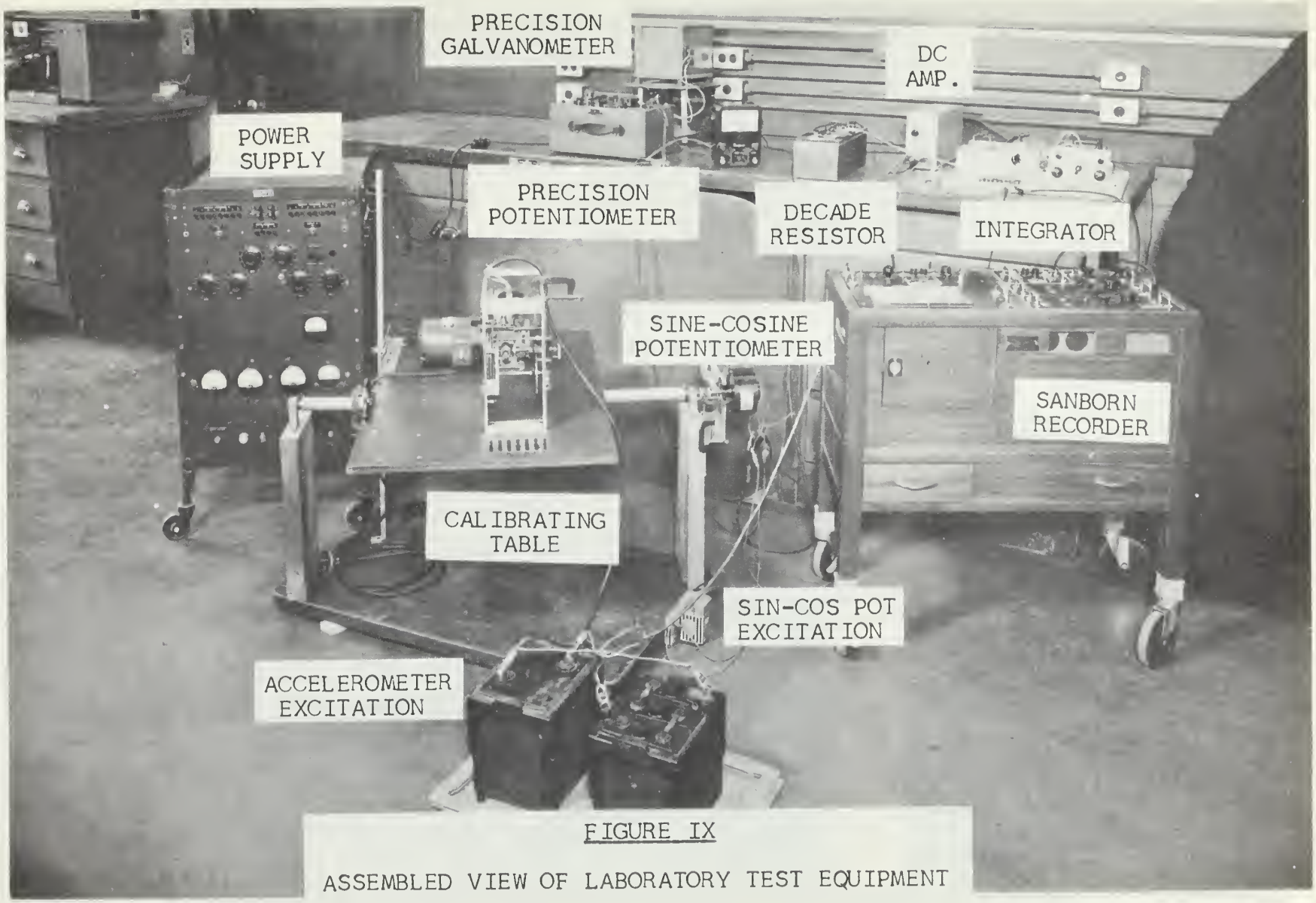

FIGURE IX

ASSEMBLED VIEW OF LABORATORY TEST EQUIPMENT

FIGURE X

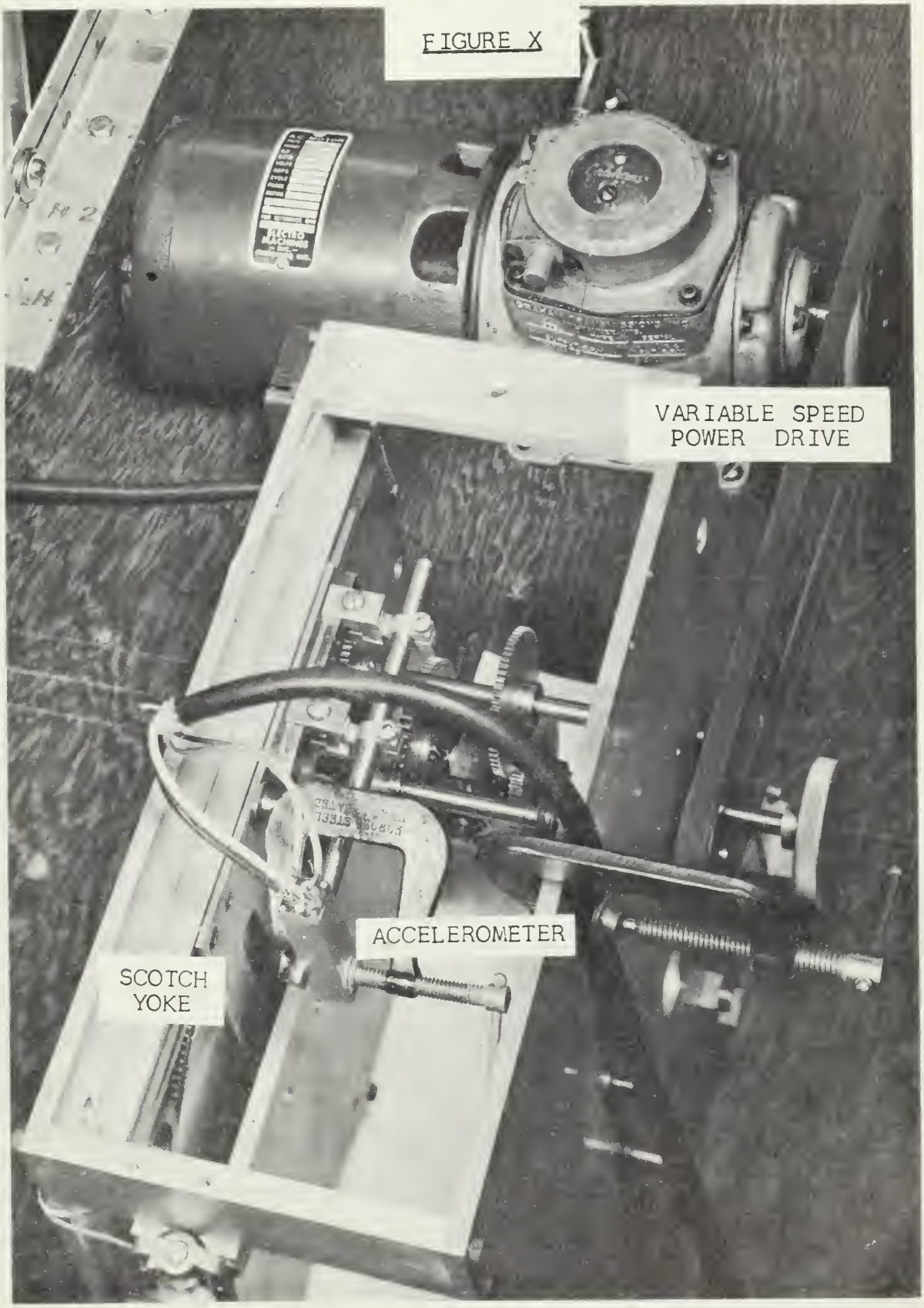

ASSEMBLED VIEW OF ACCELEROMETER, SCOTCH YOKE, AND POWER DRIVE

The different amplitudes thus obtained were normalized with respect to that for 76 rpm and plotted on Figure XXXII.

The frequency response, Figure XXXIII, of the double integrator was calculated from this same recording by scaling the output in millivolts from the Sanborn recorder data. The acceleration signal was calculated for the known acceleration amplitudes of the accelerometer by using the calibration factor for that instrument. The system gain was then divided by 100 (the Video amplifier gain) (28) in order to obtain the gain of the double integrator.

4. Establishment of the Drift Characteristic of the Double Integrating Summing Amplifier.

The experimental setup for this test was the same as that described for test number three. There is little need here for amplifying detail except to point out that the test was run for ten minutes, and the combination of yoke speed (76 rpm) and displacement (4.763 inches) results in an acceleration of 12.5 fps^2 which is the predicted maximum acceleration.

5. Dynamic Gravitational Error Compensation of the Linear Accelerometer Signal at Fixed Angles of Inclination.

The experimental setup was once again quite similar to that described for test number three, only this time it included the sine-cosine potentiometer circuitry, which may be seen by an inspection of Figure XI.

The essential steps carried out during this test are (a) the outputs of the accelerometer, and the sine-cosine potentiometer were established at zero with the table horizontal, (b) the table was rotated to an angle of forty-five degrees, and the accelerometer output was measured, (c) by varying the decade resistor, the magnitude of the

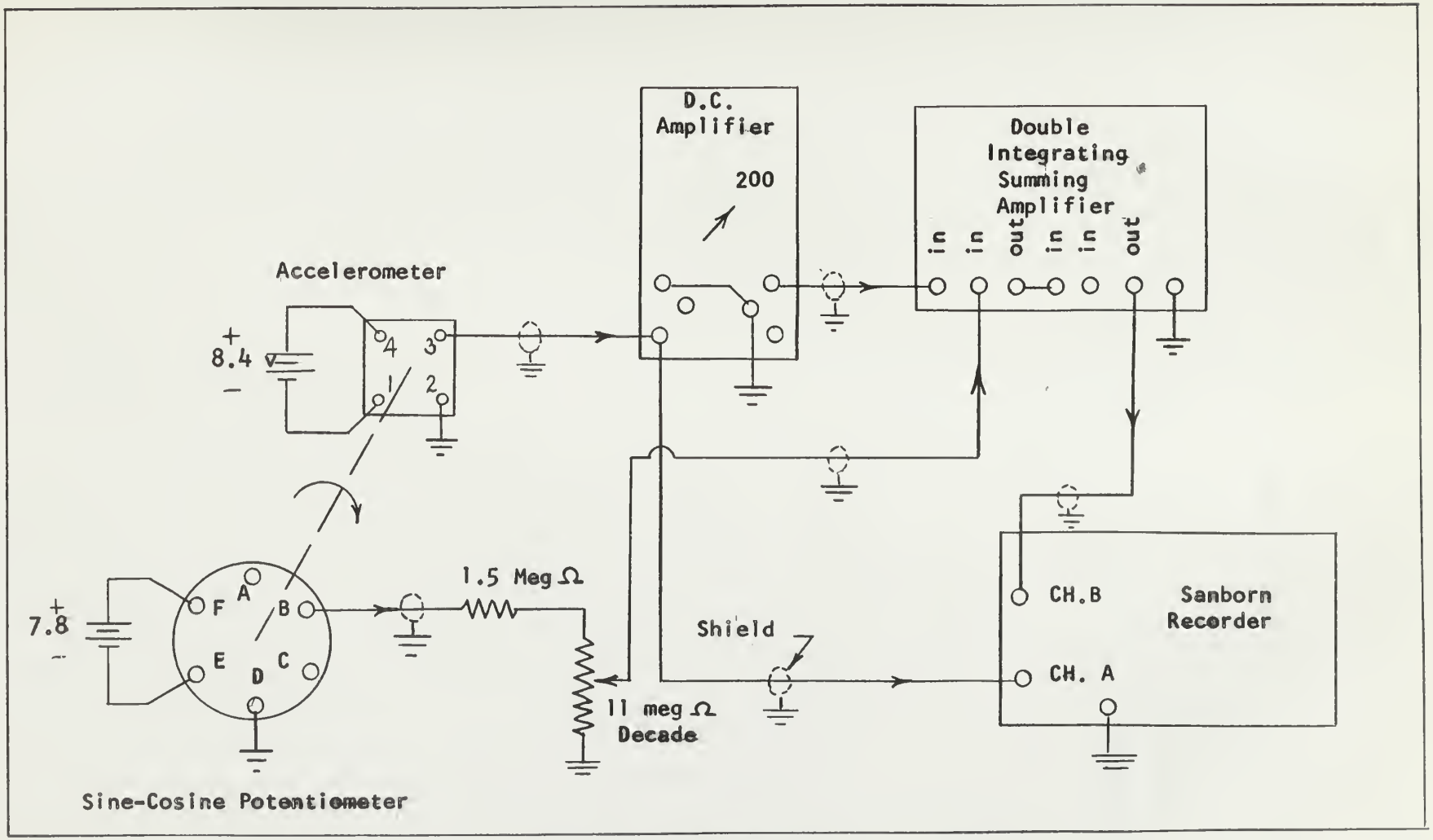

FIGURE XI

Dynamic Gravitational Error Compensation

voltage divider pickoff was made the same as that of the accelerometer output, and (d) with the system thus adjusted the Scotch Yoke was activated, subjecting the accelerometer to a known acceleration amplitude of 12.5 fps^2. It was intended to rotate the calibrating table back into the horizontal plane, at five degree intervals, while noting the system output. However, the test results were unsuccessful and, due to lack of time, this testing procedure was discontinued.

III. RESULTS

Sensing Elements

a. Linear Motions: Linear Accelerometer, unbonded strain gage type.

Statham Laboratories, Inc.

Natural Freq.: 21-40 cps.

Transduction: Resistive, complete balanced bridge

Excitation: D.C. or A.C. 9-11 volts

Output: 17-35 mv per g.

Damping: 0.7 ($\pm$ 0.1) of critical at room temp.

Ambient temp. limits: -40° to $+ 150^{\circ}$F.

Max. allowable static acceleration: 3 times rated range

Response to transverse acceleration: .02 g per g.

Non-linearity and hysteresis: 1% of full scale excursion.

Weight: 35 grams to 13.5 ounces

Size: $3\frac{1}{2}$" x 2" x $1\frac{1}{4}$" or smaller.

b. Angular Motions: Miniature Rate Gyroscopes.

Manufacturer's Data

	Minneapolis Honeywell GN-40	or	U.S. Time Corp. UST #400
Full scale rate:	400°/sec.		± 400°/sec.
Angular momentum:	38,600 gm-cm^2/sec.		32,600 gm-cm^2/sec.
Undamped natural freq:	76 cps.		88 cps.
Damping Ratio:	0.6		0.7 or to suit
Excitation:	6.3 v, 400 cps, 2 phase 26 v, 400 cps, 2 phase		6.3 v, 400 cps, 2 phase 26 v, 400 cps, 2 phase
Full scale gimbal deflection:	3.0°		2.6°
Acceleration time:	15 sec.		15 sec.
Full scale output:	5.6 v. (RMS)		5.6 v. (RMS)
Sensitivity:	14 mv/deg/sec.		14 mv/deg/sec.
Threshold & Resolution:	.01 degrees/sec.		.02 degrees/sec.
Inertia Ratio:	.00045 sec.		.0004 sec.
Type of Pickoff:	Variable Reluctance		Variable Reluctance
Linearity:	0.1% to ½ range 2% to full range		0.1% to ½ range 1% to full range
Ambient Temp. Range:	-67° to + 185°F		-67° to 212F.
Shock or Linear Acceleration:	Up to 100 g.		>200 g.
Linear Vibration:	Up to 10 g, 0 to 2000 cps.		25-30 g.
Size:	1" diam. x 2¼" long		.94" diam. x 2 3/16" long.
Weight:	3.8 ounces		3.5 ounces.

FIGURE XII

Linear Accelerometer Direct Axis Error Due To Angular Velocities and Accelerations

(For Tabulation of Data See Appendix B)

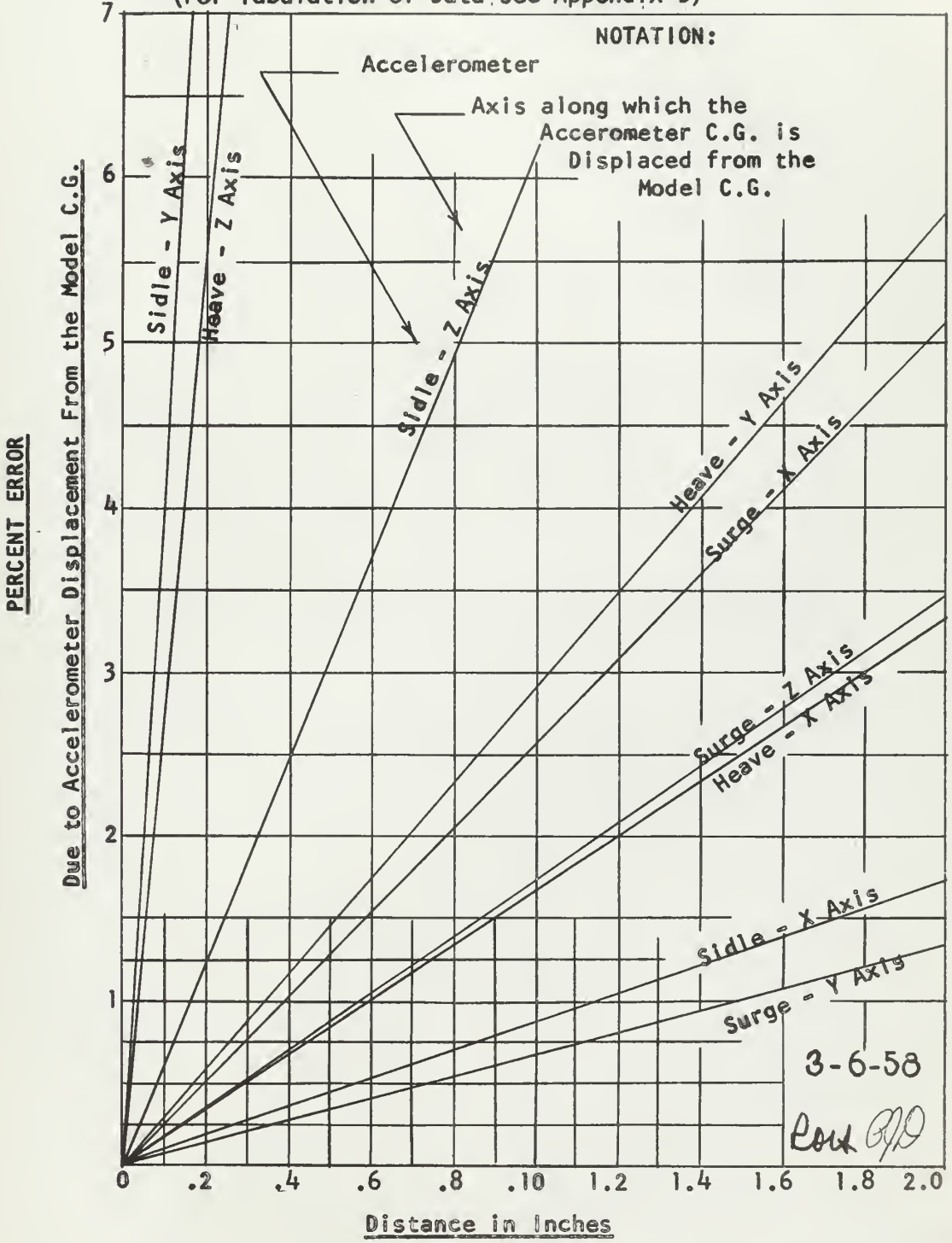

FIGURE XIII

Accelerometer Arrangement

Ref.: STATHAM INSTALLATION DWGS 6620 and 6623

Note: All Dimensions are in Inches

TOP VIEW Full Scale

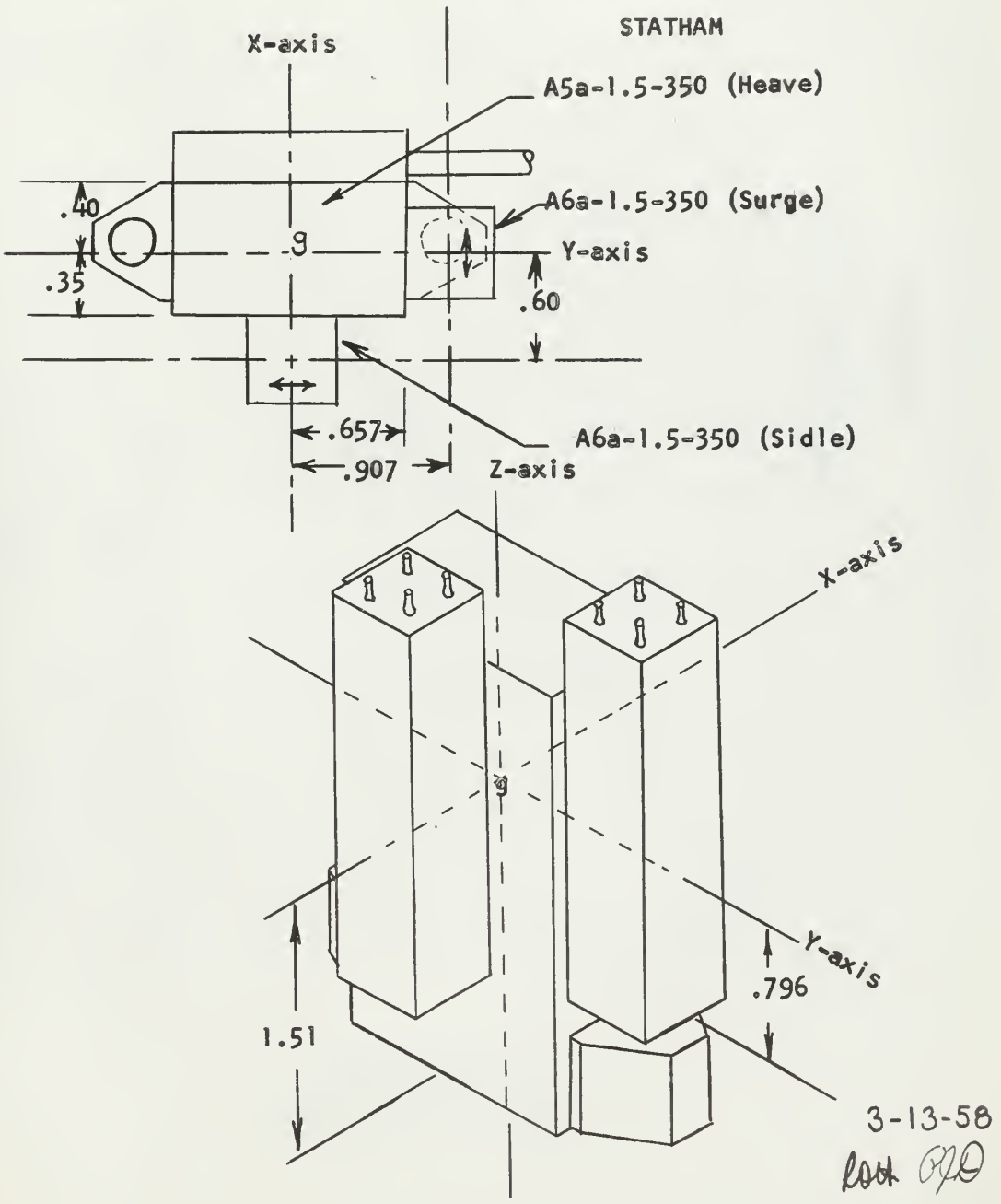

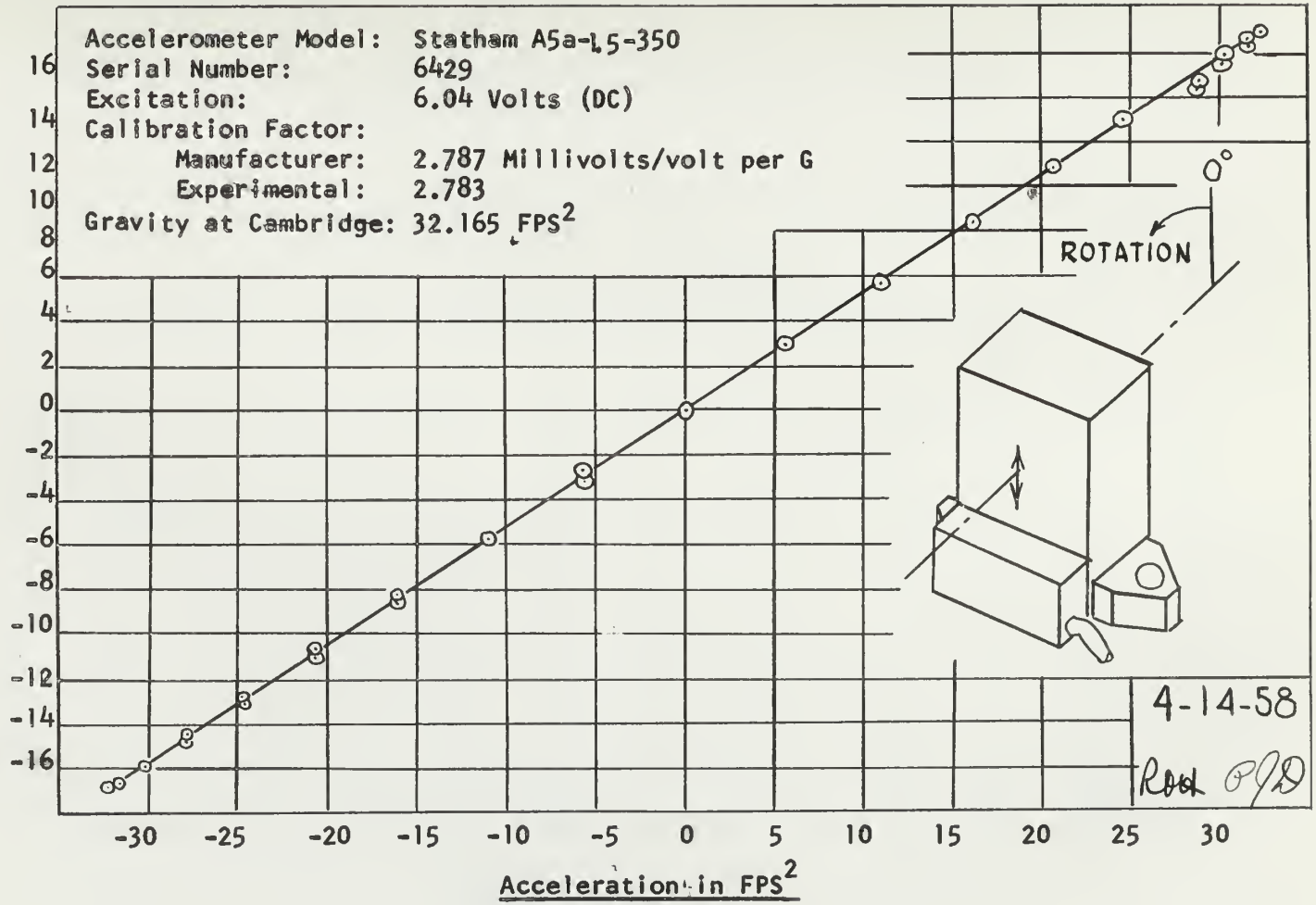

FIGURE XIV

Static Calibration of Accelerometer A5a-1.5-350

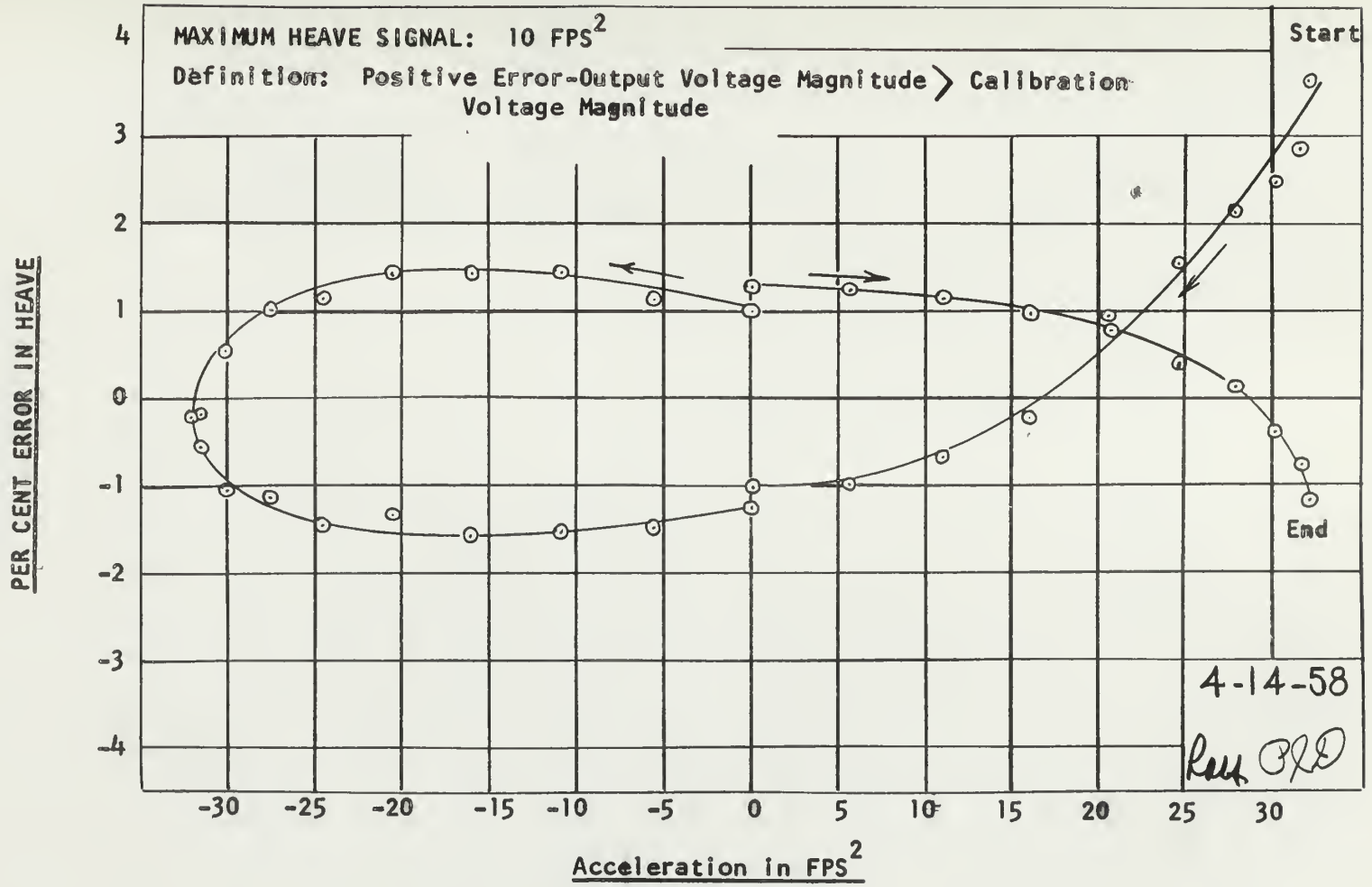

FIGURE XV

Linearity and Hysteresis Error of Accelerometer A5a-1.5-350

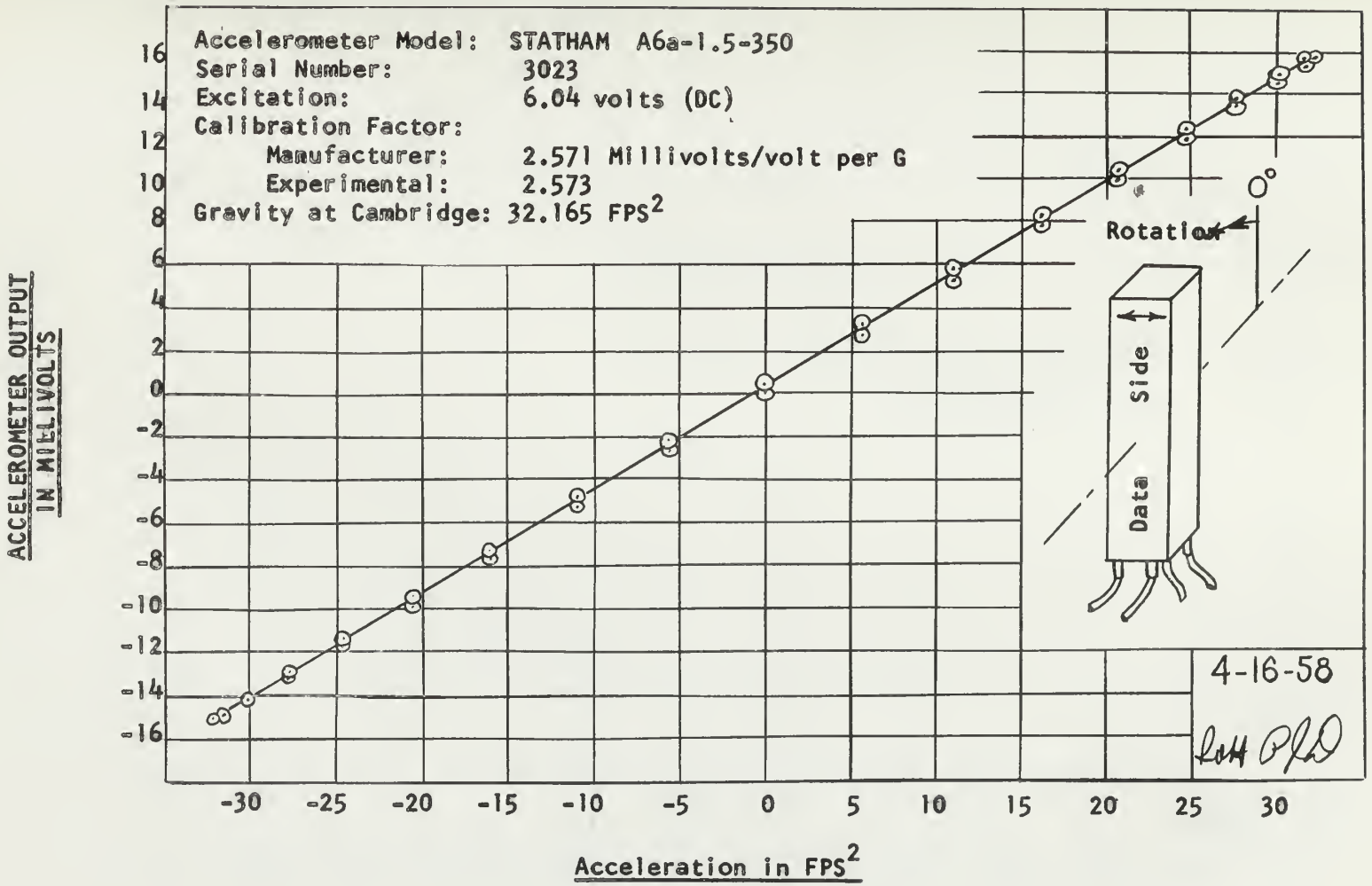

FIGURE XVI

Static Calibration of Accelerometer A6A-1.5-350 (3023)

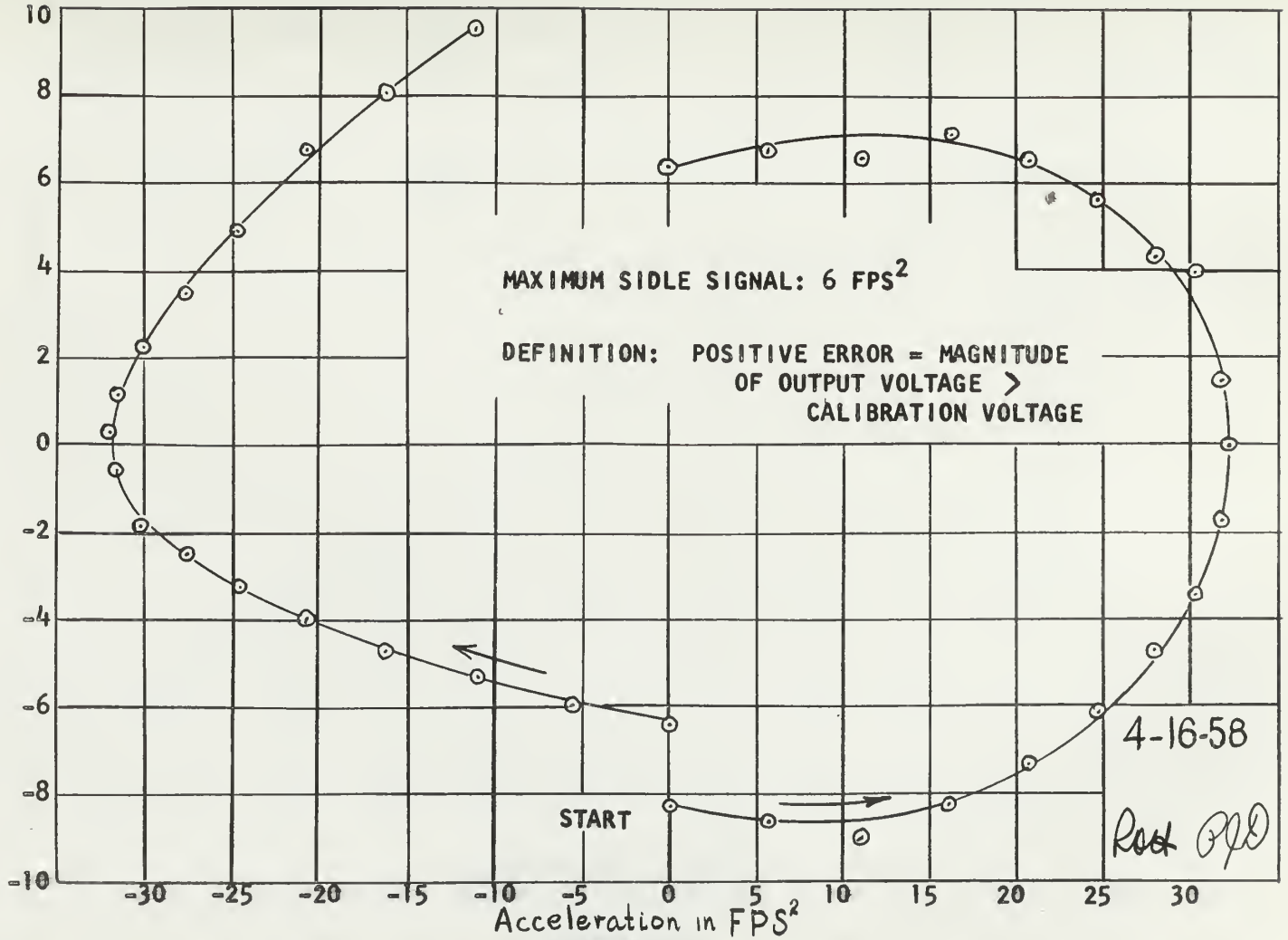

FIGURE XVII

Linearity and Hysteresis Error of Accelerometer A6a-1.5-350 (3023)

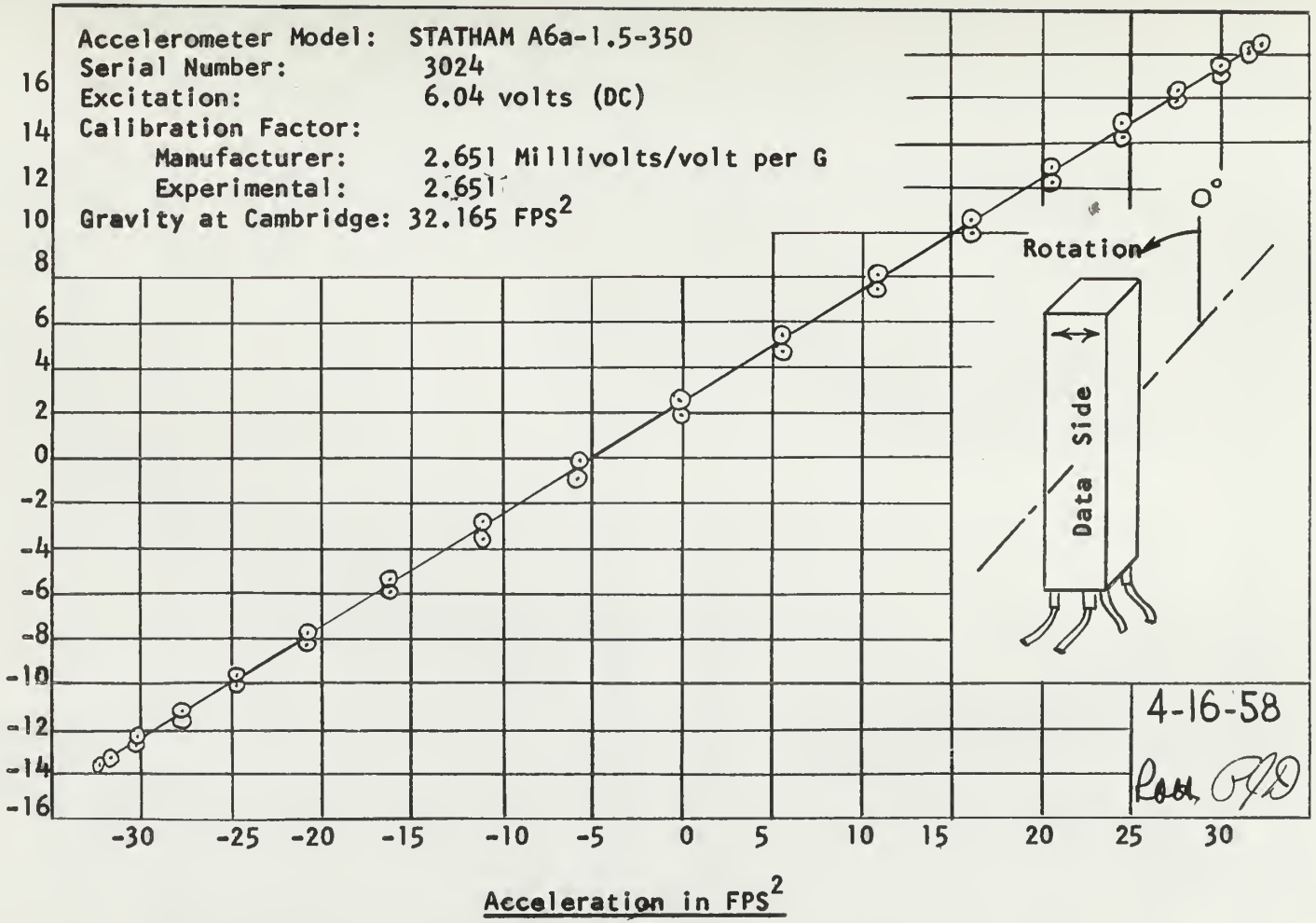

FIGURE XVIII

Static Calibration of Accelerometer A6a-1.5-350 (3024)

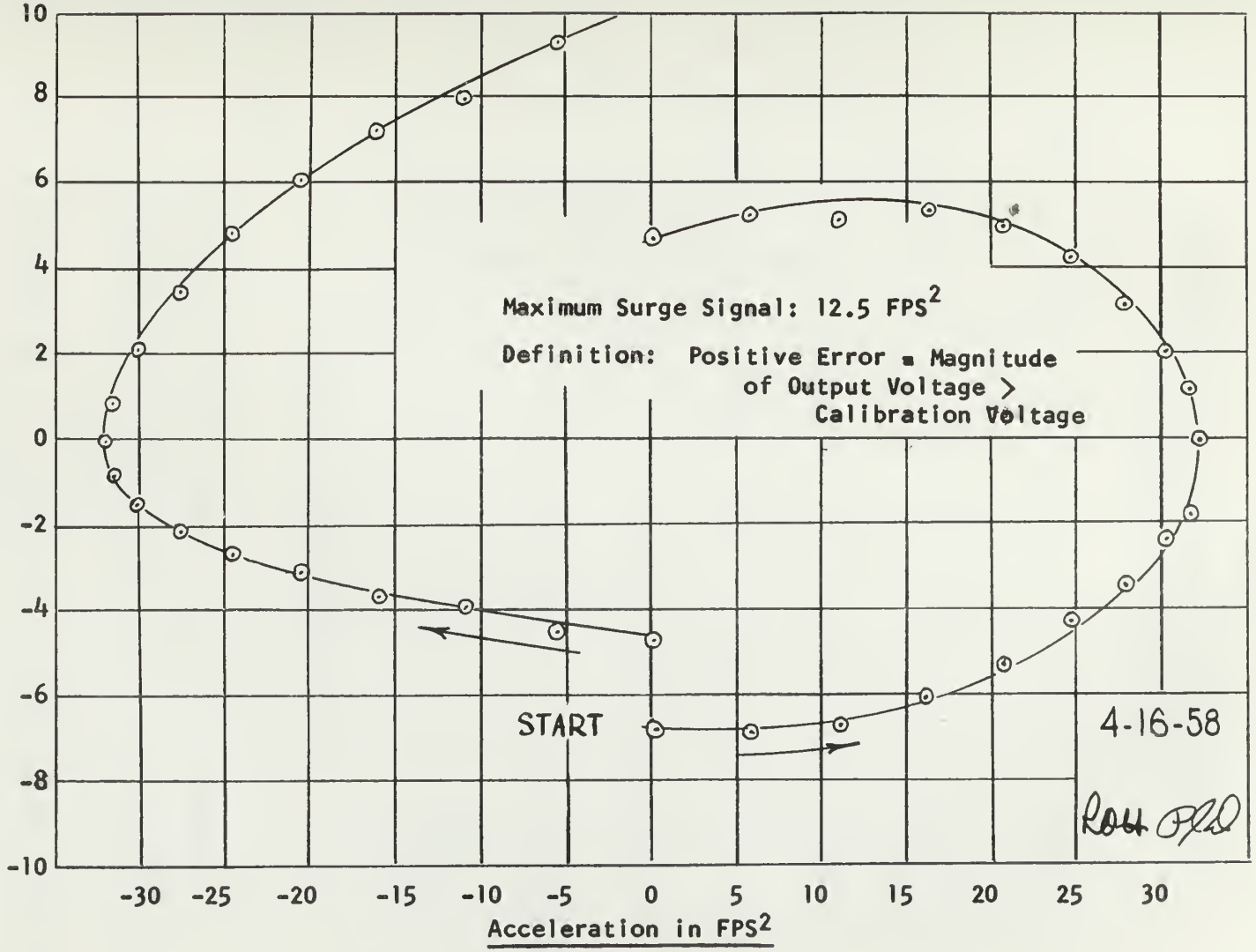

FIGURE XIX

Linearity and Hysteresis Error of Accelerometer A6a-1.5-350 (3024)

FIGURE XX

Maximum Error in Statham Linear Accelerometers
Due to Linear Accelerations Normal to
The Indicated Sensitive Axis*

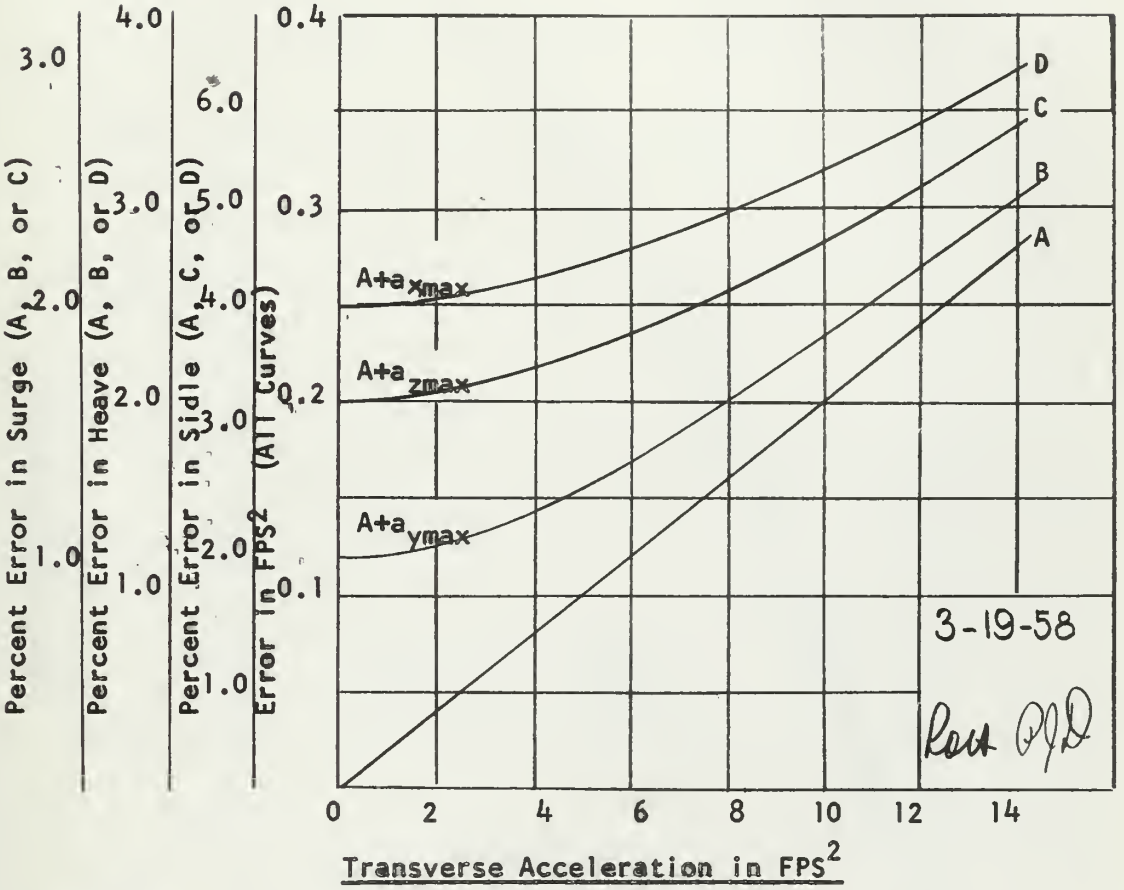

LEGEND:

A - Any acceleration normal to the indicated axis

B - Vector sum of A (heave or surge) and maximum sidle signal

$$B = \sqrt{A^2 + 36} \qquad (a_{y_{max}} = 6 \text{ FPS}^2)$$

C - Vector sum of A (surge or sidle) and maximum heave signal

$$C = \sqrt{A^2 + 100} \qquad (a_{z_{max}} = 10 \text{ FPS}^2)$$

D - Vector sum of A (heave or sidle) and maximum surge signal

$$D = \sqrt{A^2 + 156.2} \qquad (a_{x_{max}} = 12.5 \text{ FPS}^2)$$

* Based on Ref. (3)

FIGURE XXI

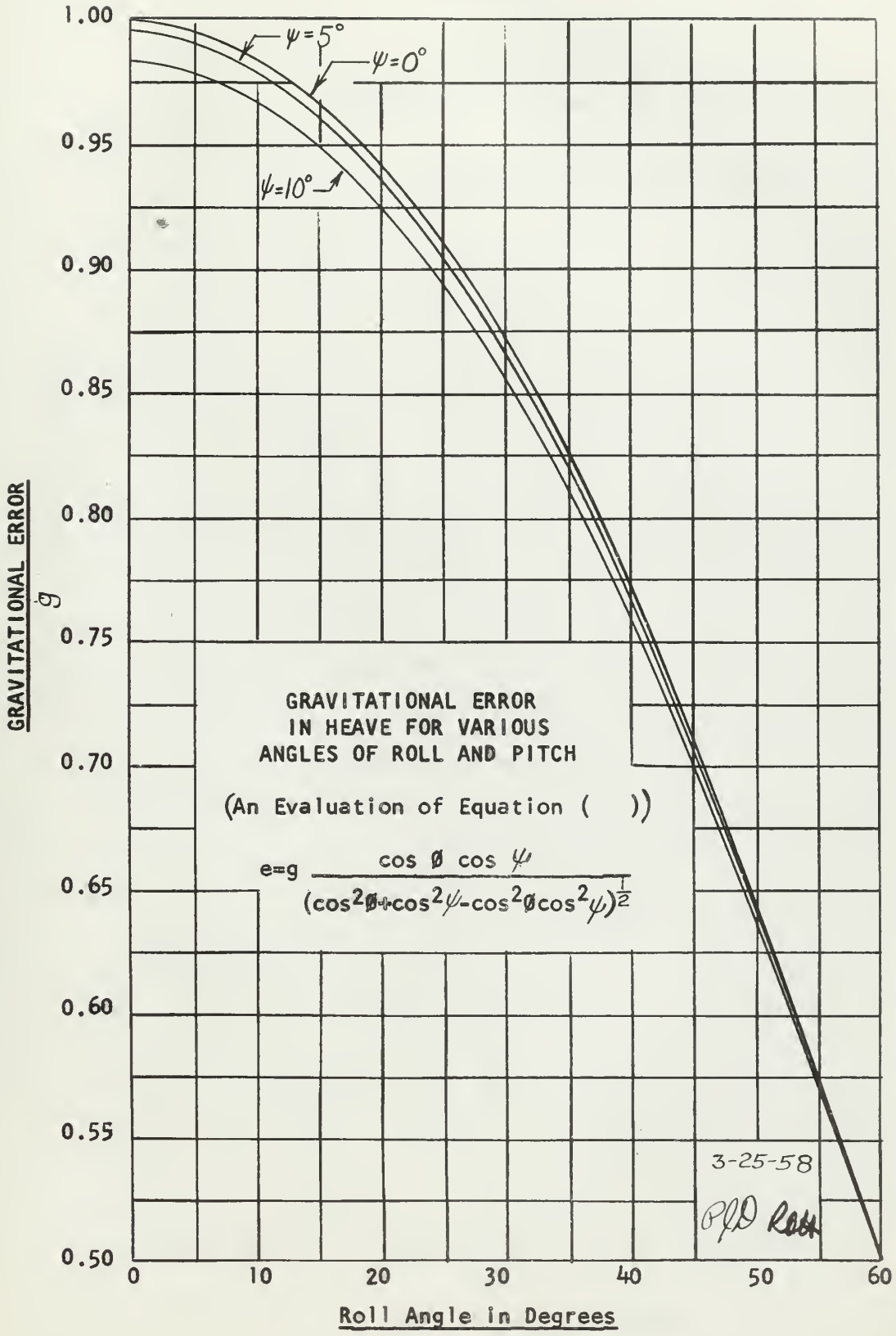
1.00
0.95
0.90
0.85
0.80
0.75
0.70
0.65
0.60
0.55
0.50
GRAVITATIONAL ERROR
g
ψ=5°
ψ=0°
ψ=10°
GRAVITATIONAL ERROR
IN HEAVE FOR VARIOUS
ANGLES OF ROLL AND PITCH
(An Evaluation of Equation ( ))
e=g cos Ø cos ψ / (cos²Ø+cos²ψ-cos²Øcos²ψ)^½
3-25-58
PJD Roll
0
10
20
30
40
50
60
Roll Angle in Degrees

FIGURE XXII

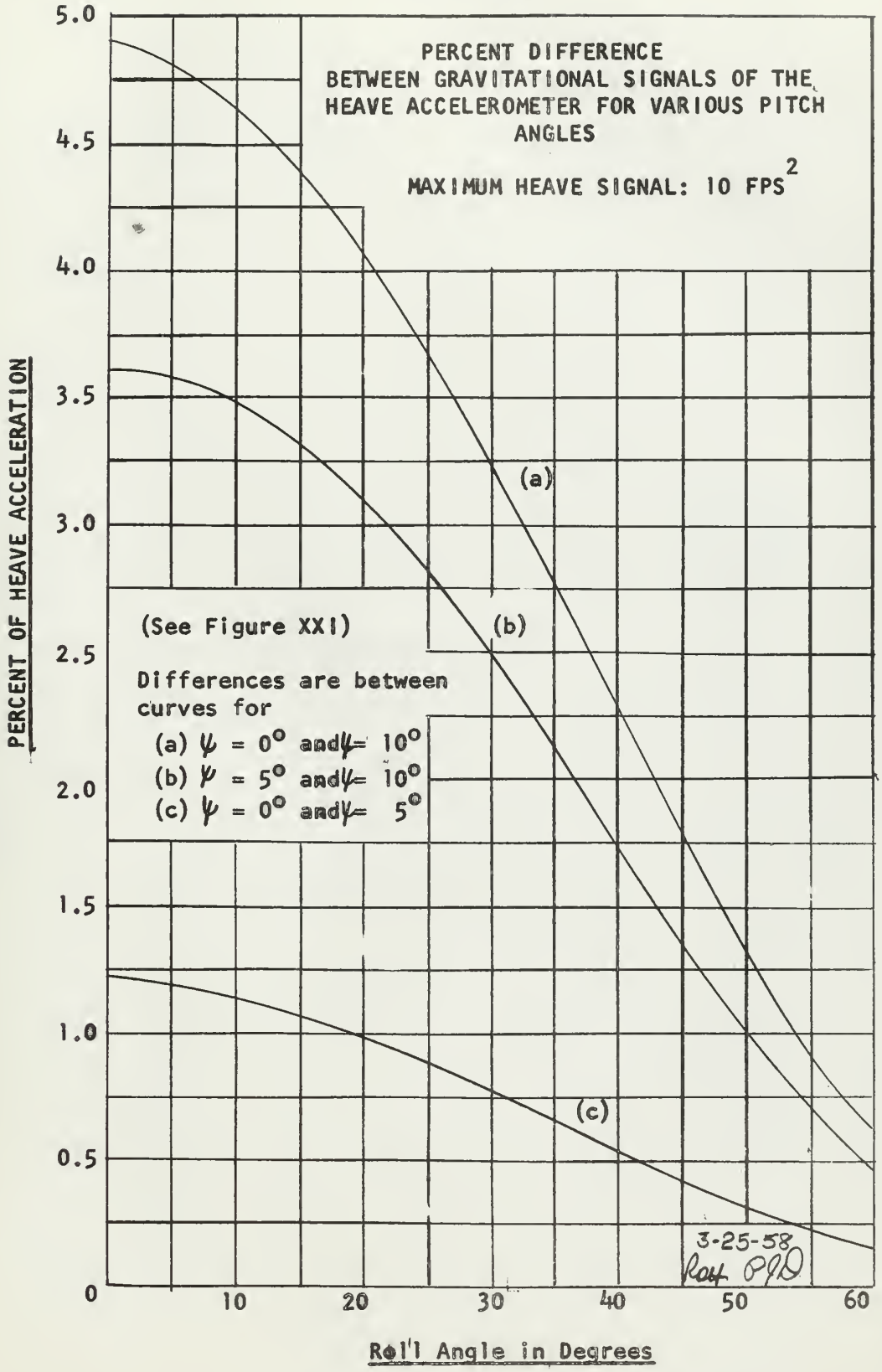
PERCENT DIFFERENCE
BETWEEN GRAVITATIONAL SIGNALS OF THE HEAVE ACCELEROMETER FOR VARIOUS PITCH ANGLES
MAXIMUM HEAVE SIGNAL: 10 FPS²
(See Figure XXI)
Differences are between curves for
(a) ψ = 0° and ψ = 10°
(b) ψ = 5° and ψ = 10°
(c) ψ = 0° and ψ = 5°
(a)
(b)
(c)
3-25-58
Roll
PERCENT OF HEAVE ACCELERATION
5.0
4.5
4.0
3.5
3.0
2.5
2.0
1.5
1.0
0.5
0
10
20
30
40
50
60
Roll Angle in Degrees

FIGURE XXIII

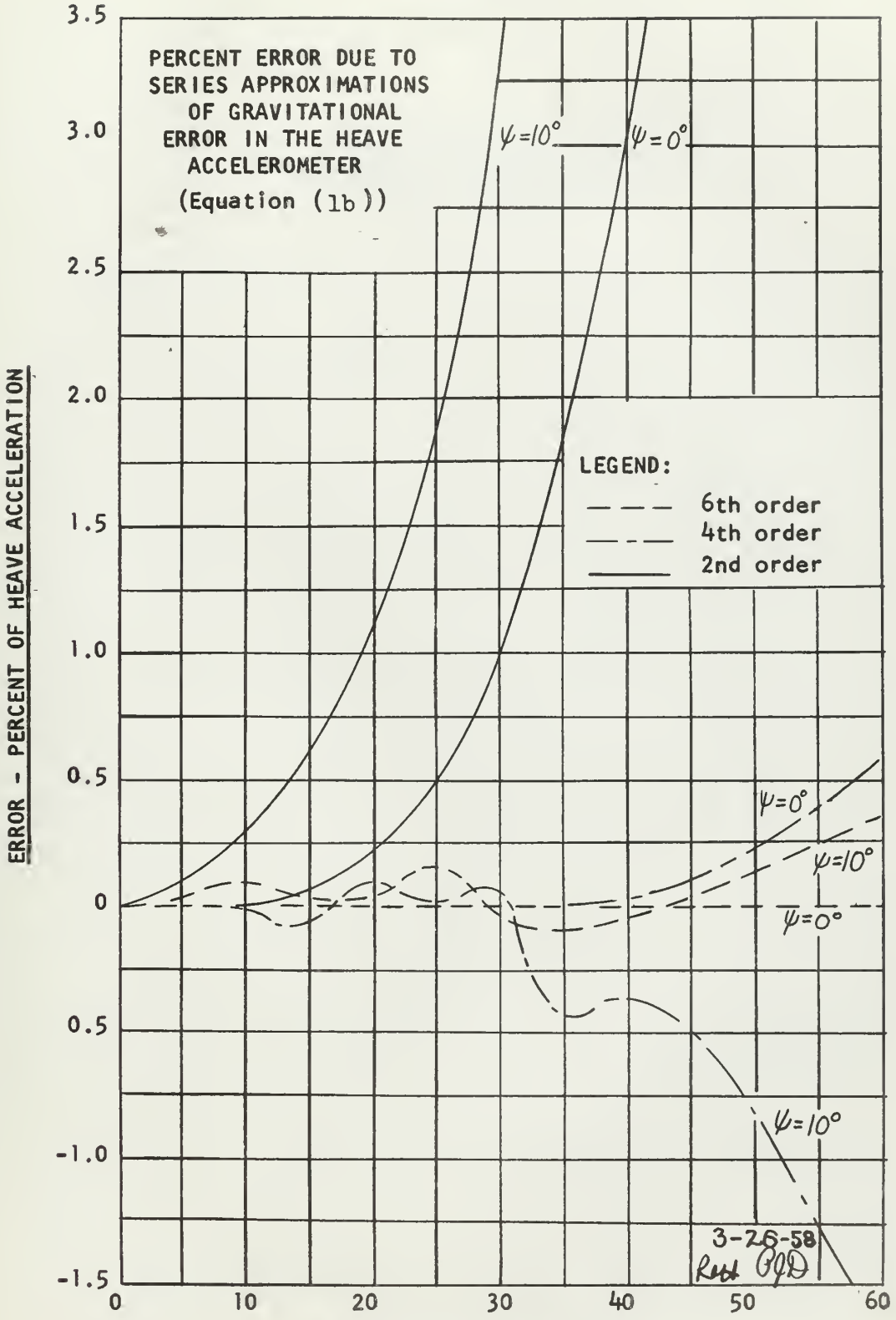

FIGURE XXIV

Error From Use of an
Approximate Trigonometric Relation
To Describe Gravitational
Error in Heave

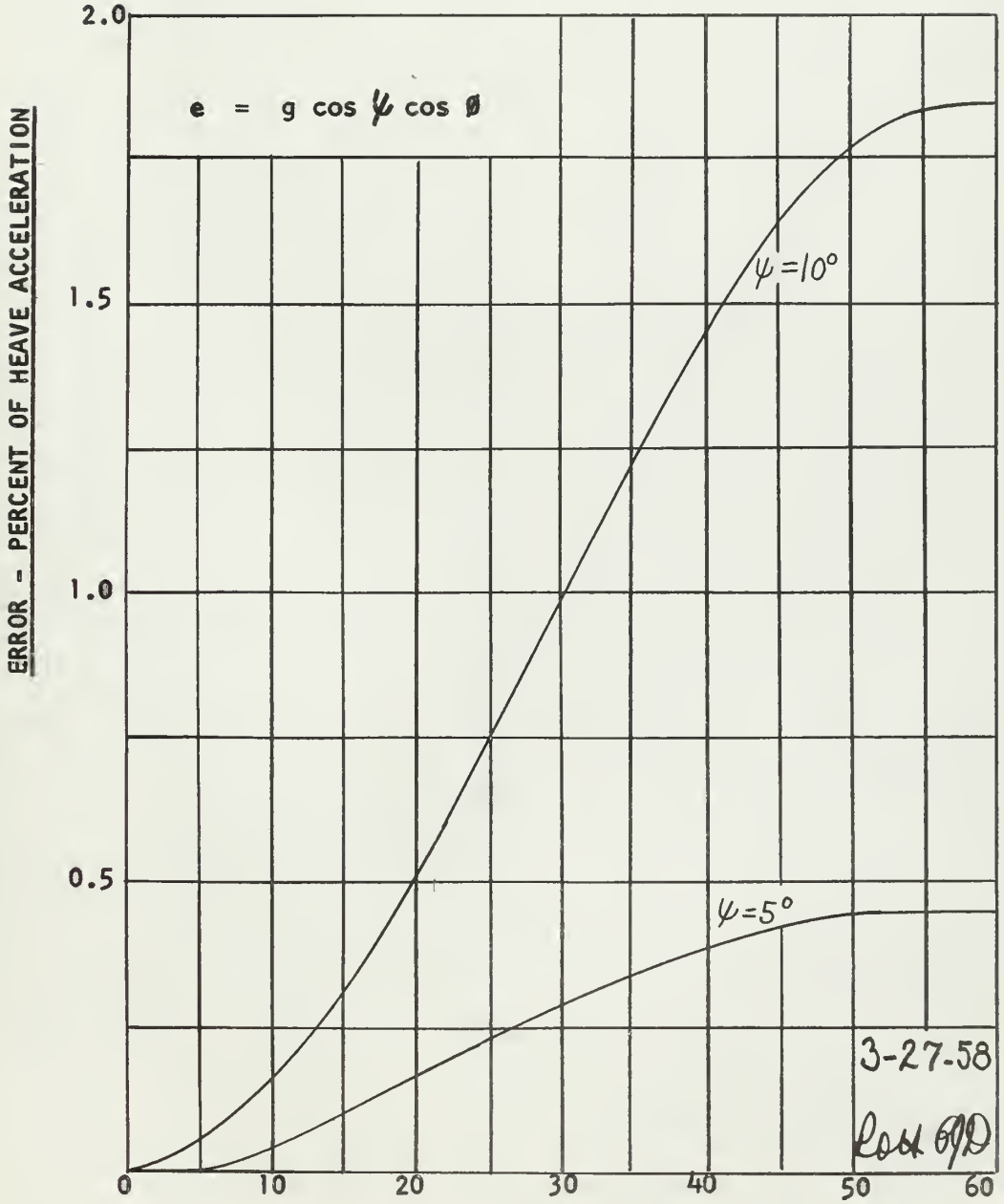

FIGURE XXV

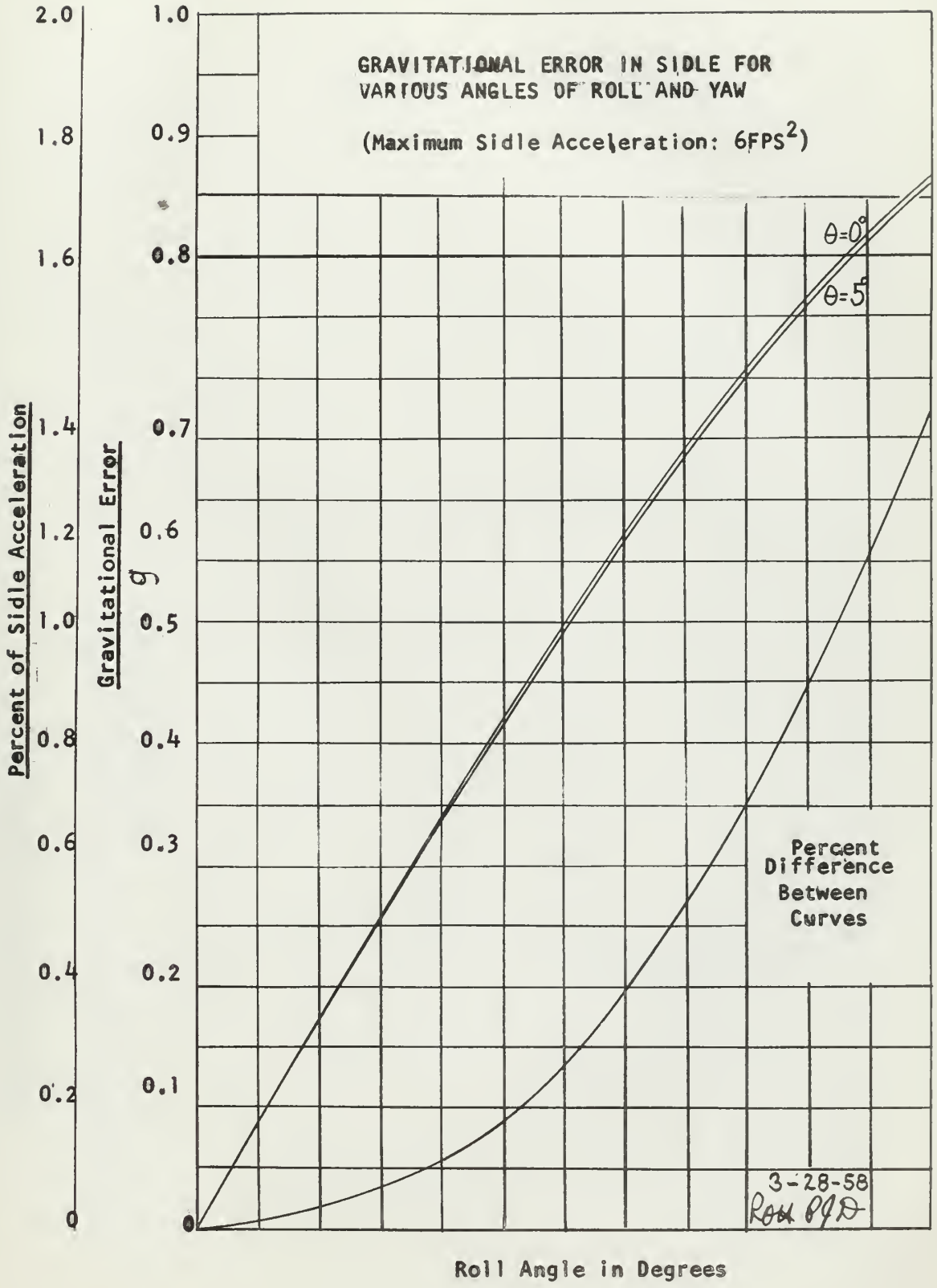
GRAVITATIONAL ERROR IN SIDLE FOR
VARIOUS ANGLES OF ROLL AND YAW
(Maximum Sidle Acceleration: 6FPS²)
θ=0°
θ=5°
Percent
Difference
Between
Curves
3-28-58
Percent of Sidle Acceleration
Gravitational Error
g
Roll Angle in Degrees
2.0
1.8
1.6
1.4
1.2
1.0
0.8
0.6
0.4
0.2
0
1.0
0.9
0.8
0.7
0.6
0.5
0.4
0.3
0.2
0.1
0

FIGURE XXVI

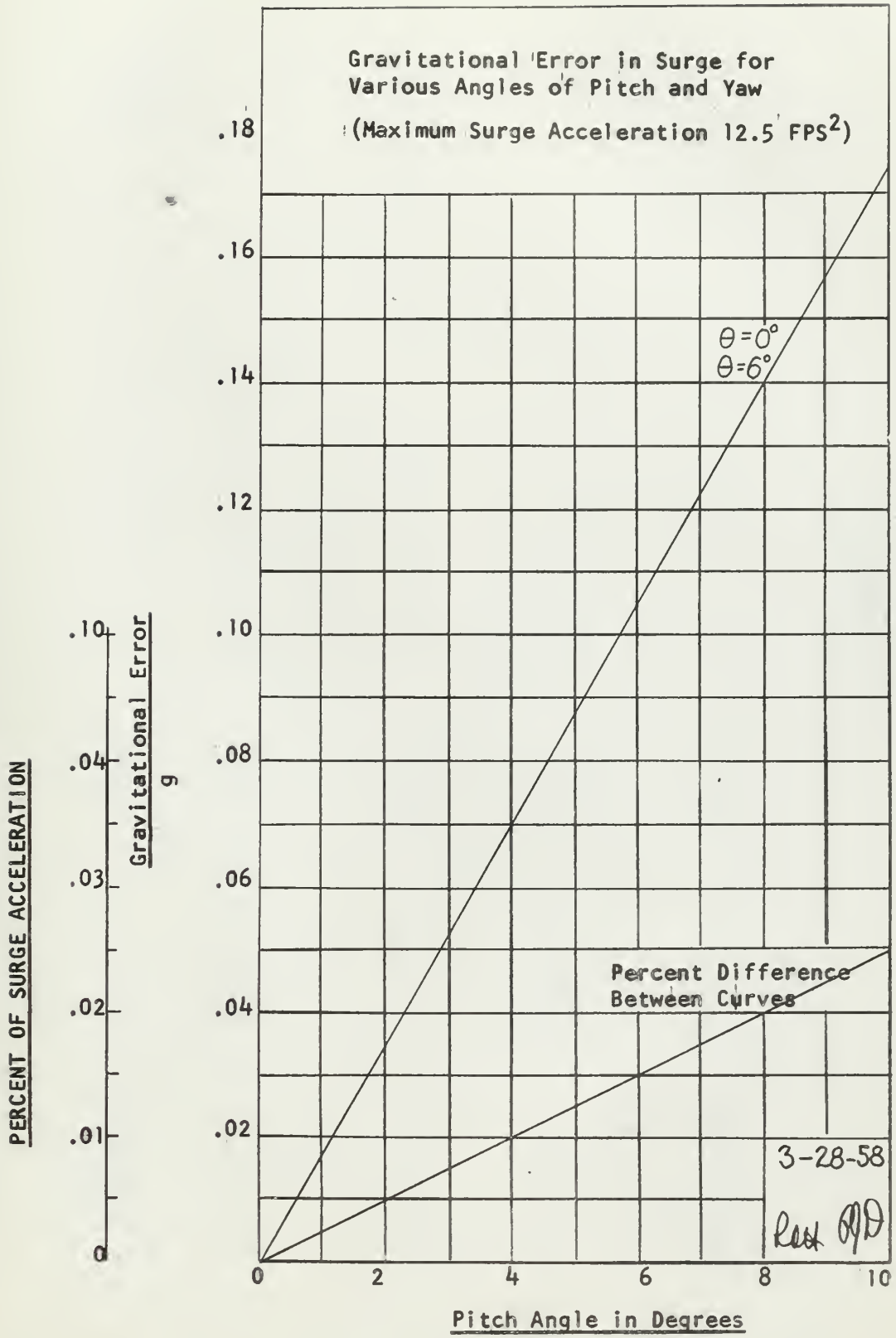
Gravitational Error in Surge for
Various Angles of Pitch and Yaw
(Maximum Surge Acceleration 12.5 FPS²)
θ=0°
θ=6°
Percent Difference
Between Curves
3-28-58
Rev RD
.18
.16
.14
.12
.10
.08
.06
.04
.02
0
2
4
6
8
10
Pitch Angle in Degrees
PERCENT OF SURGE ACCELERATION
Gravitational Error
g
.10
.04
.03
.02
.01
0

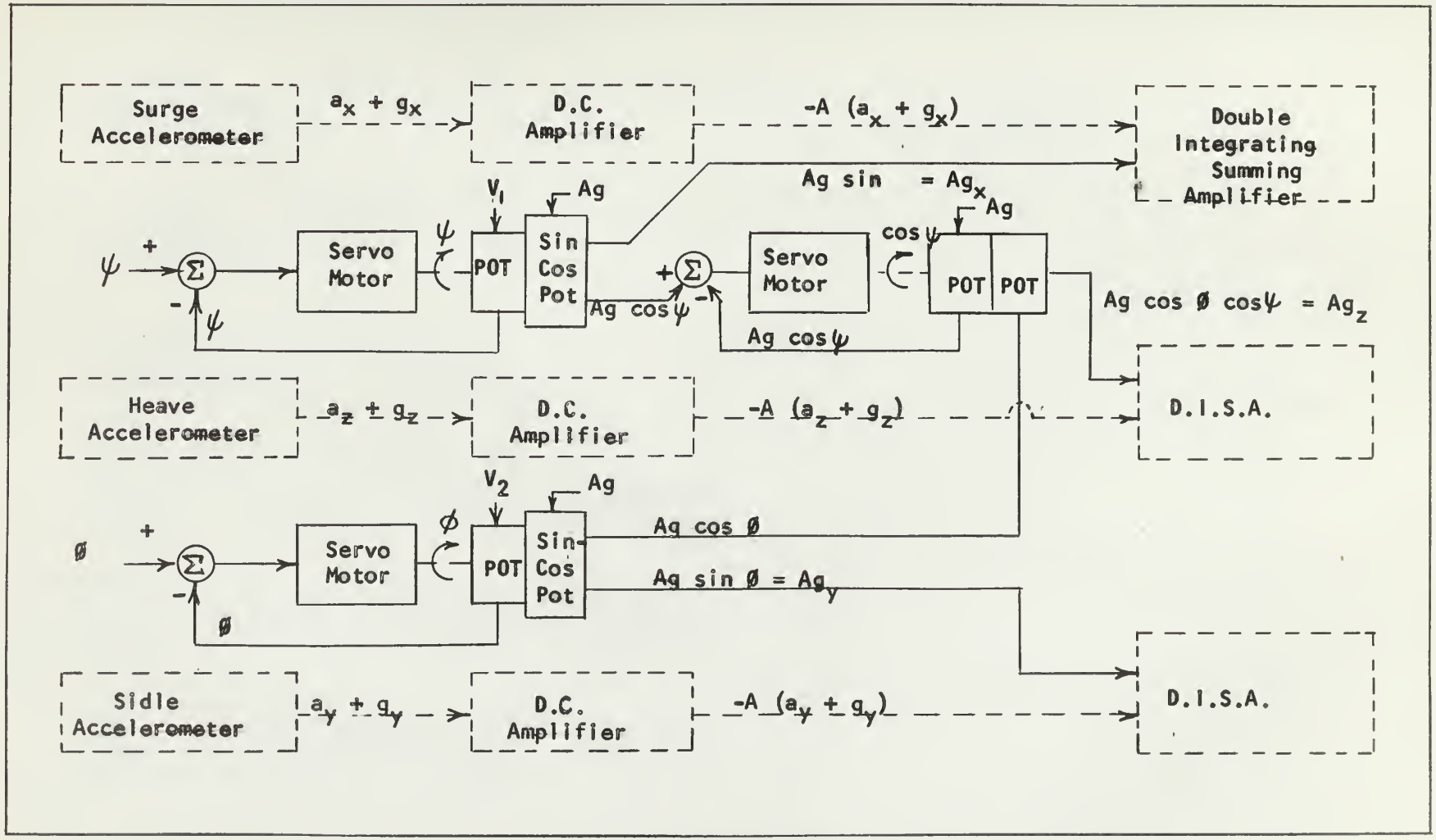

FIGURE XXVII

Proposed Gravitational Error Compensation System

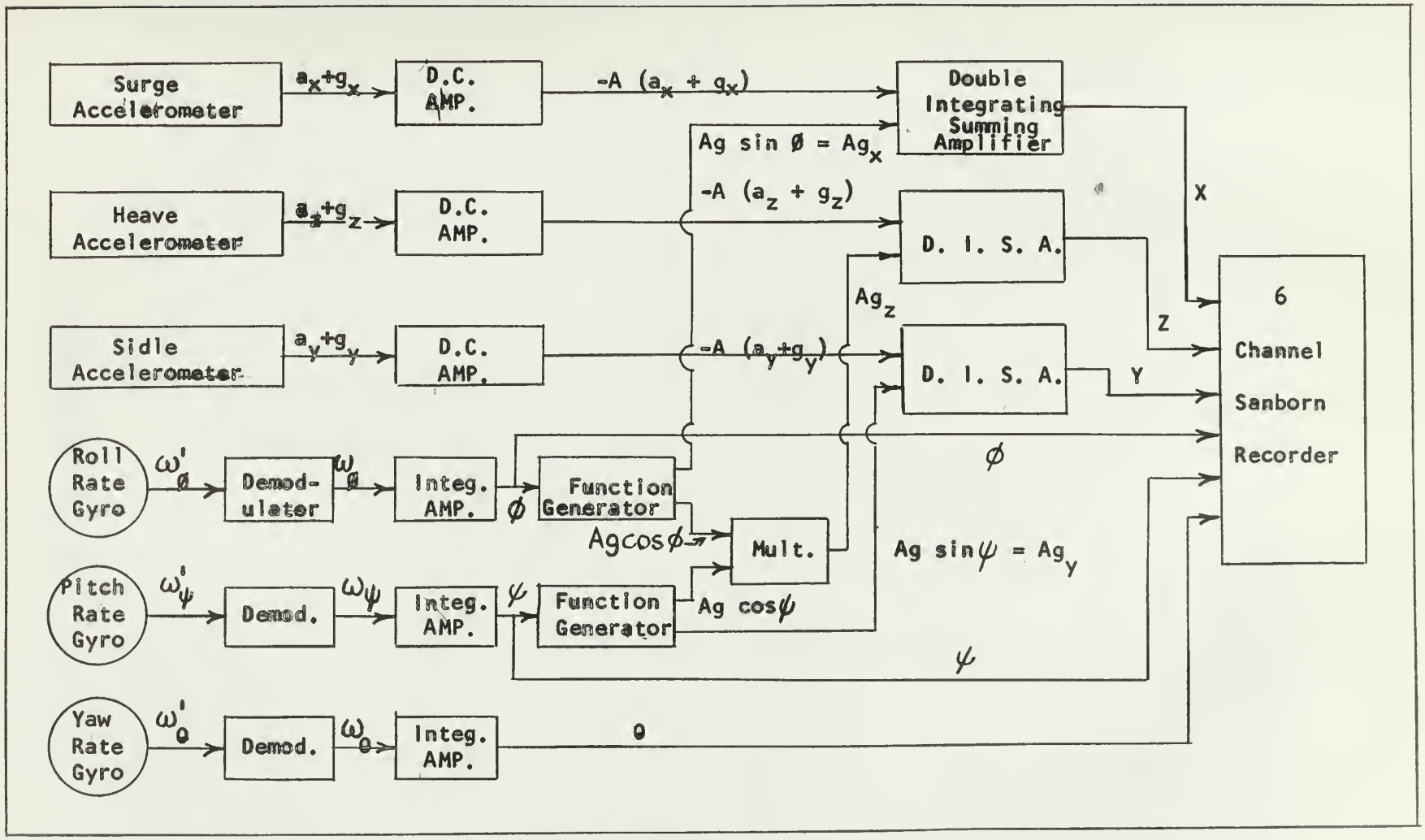

FIGURE XXVIII

Schematic Diagram of Proposed Sensing System

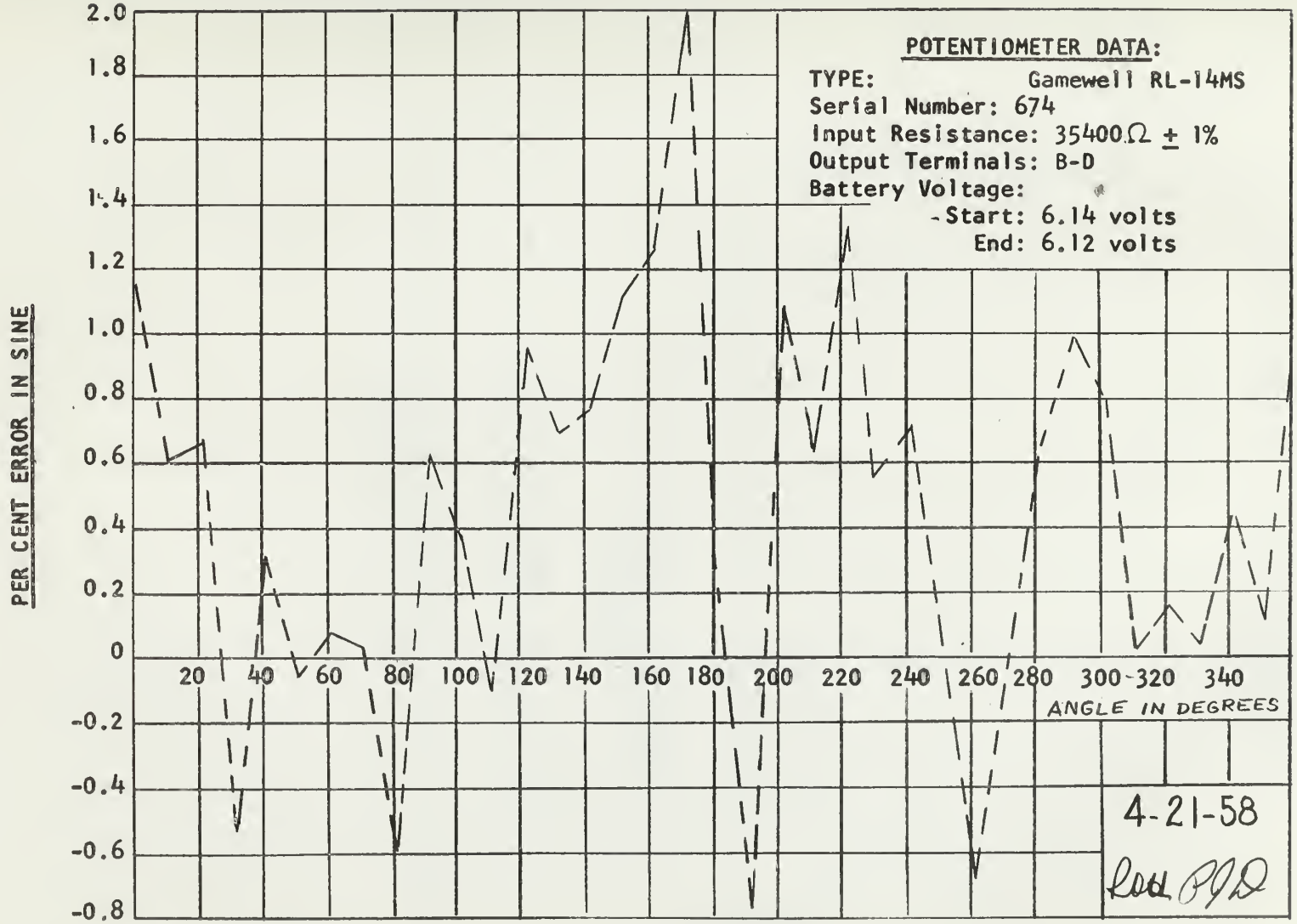

FIGURE XXIX

Calibration of Sine-Cosine Potentiometer

FIGURE XXX

Ability of the Sine-Cosine Potentiometer
To Null Gravitational Errors

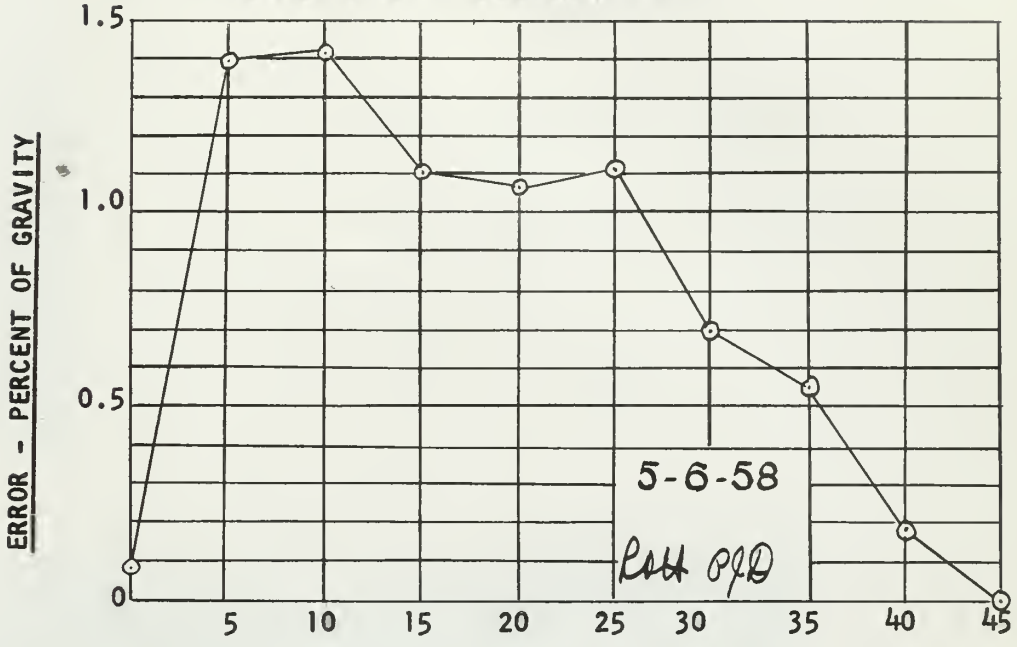

Accelerometer: Statham A6a-1.5-350; Ser. No. 3023
Excitation: 8.4 Volts (D.C.)

Sine-Cosine Potentiometer: Gamewell RL-14MS: Ser. No. 674
Excitation: 7.8 volts (D.C.)

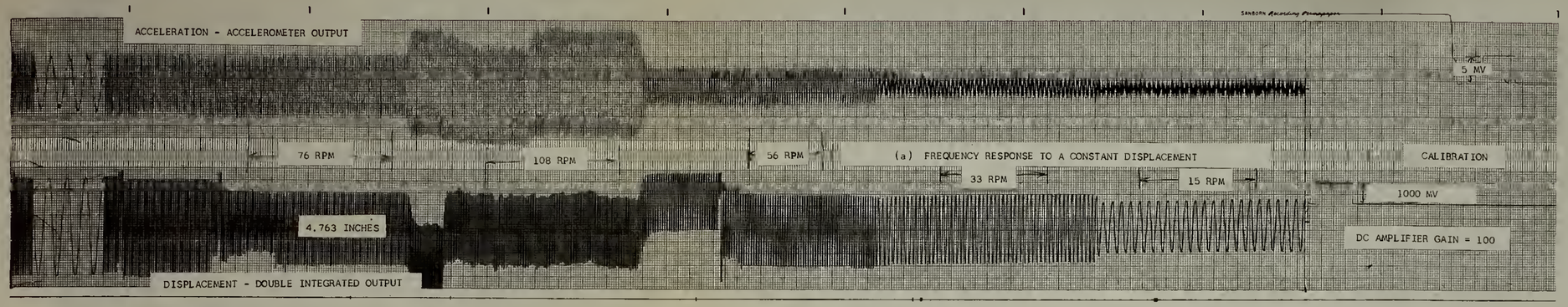

FIGURE XXXI

SANBORN RECORDINGS

(a) DOUBLE INTEGRATOR RESPONSE TO A CONSTANT DISPLACEMENT INPUT

(b) DRIFT CHARACTERISTIC OF THE DOUBLE INTEGRATING SUMMING AMPLIFIER

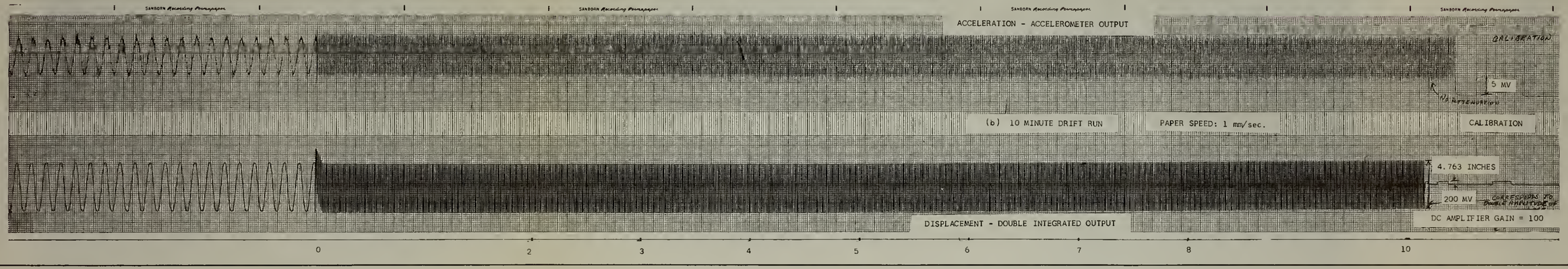

FIGURE XXXII

Double Integrator Response to a
Constant Displacement Input

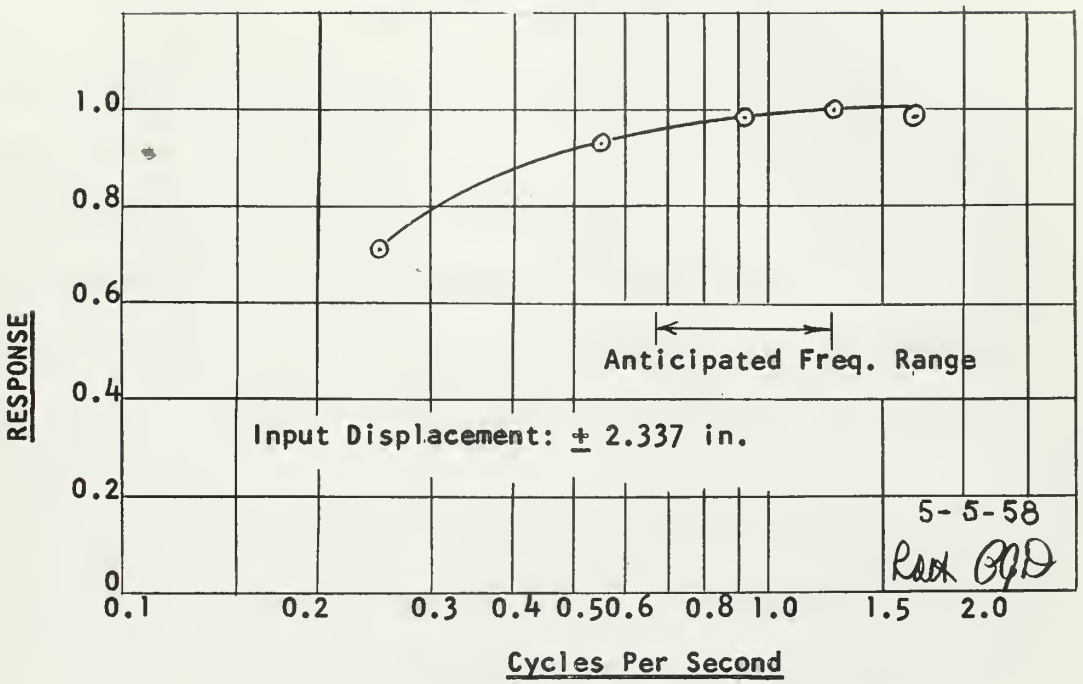

FIGURE XXXIII

Frequency Response of Double Integrating Amplifier

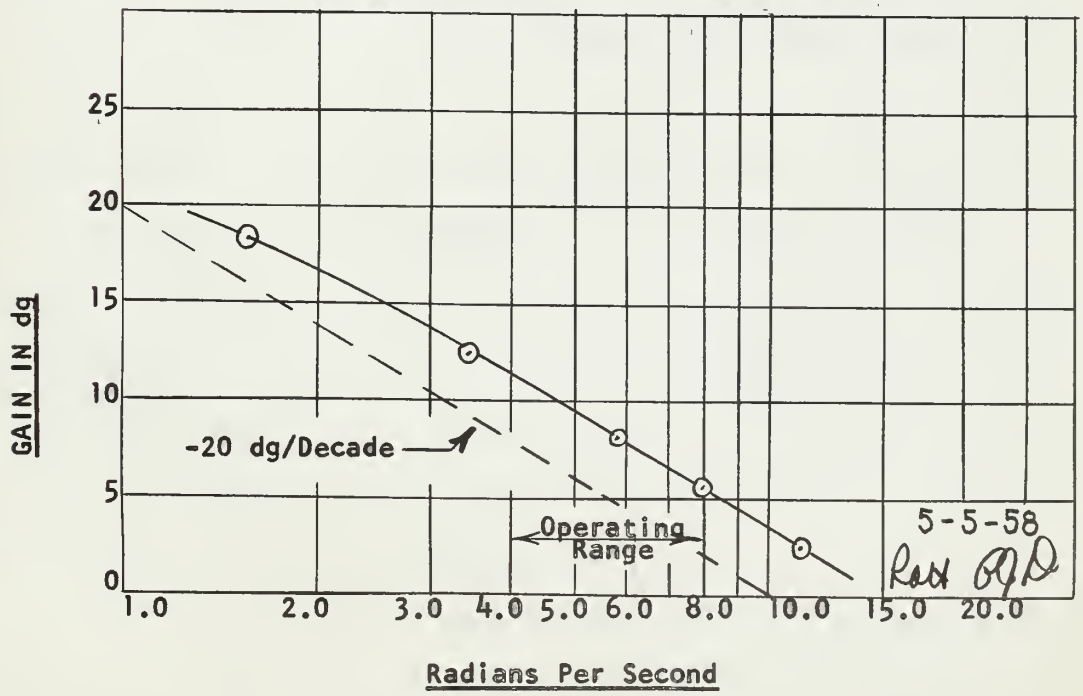

IV. DISCUSSION OF RESULTS

A. Selection of Sensing Elements

The sensing elements chosen fall well within the space and weight restrictions of the model carried equipment. It is felt that these instruments represent the optimum selection of commercially available components. The overall system is not the least complex that could have been designed, but the space and weight restrictions of the model carried components have imposed this compromise.

The time required for delivery did not permit the purchase of the rate gyros. However, a brief analysis of possible gyro errors shows the following:

1. Hysteresis is .05% of full scale or 0.2° per second. The smallest design magnitude of angular velocity is that for yaw (39.2° per second). Therefore, the largest possible error is only .51%.
2. Linearity (to 200° per second) is 0.1% of full scale or 0.4° per second. The largest possible error (yaw) would be 1.02%.
3. Variation of sensitivity with temperature is .02% per °C. A 50° variation would introduce only 1% error and temperature variations of this nature are not anticipated.

In view of the above, it is felt that either the Golden Gnat 40 (10) or the UST #400 (9) would provide signals well within the error limitations. Significant errors, if present, would arise from other components in the particular system.

U. S. Time Corporation has advertised telemetering packages with D.C. output and 3 axis control packages (9). It is recommended that

these be investigated further and perhaps applied to this system.

From an inspection of Table II, it is apparent that the only linear accelerometers which meet stated system specifications are the strain guage type and the differential transformer type. The unbonded strain guage type (3) was selected in lieu of the differential transformer after a general consideration of the type of power supply required by the two instruments. It was felt that the 400 cps carrier supply required for the differential transformer would be subject to the usual frailties of regulated power supplies (17), and might unnecessarily complicate the overall system.

Figure XII played a very important role in choosing specific accelerometers as well as locating them within the package. This method of analysis is rather unique and useful. Having once established the anticipated angular accelerations, a simple calculation (page 86) will define this plot and show at a glance the best arrangement along the axes for accelerometers in the package, the minimum errors being governed only by the physical dimensions of the accelerometers. Figure XIII shows the result of just such an analysis. Other combinations of accelerometers approached this minimum error but were discarded because the output range of the sensing elements was smaller. The A5a-1.5-350 accelerometer senses heave, the priority linear signal. It is therefore located at the center of gravity to eliminate all errors due to roll and pitch accelerations. It is also the best choice in shape to allow the other two to be located as close as possible to the center of gravity of the model.

As the model rotates, the accelerometers sense that component of the gravitational acceleration parallel to their sensitive axes. Since the heave accelerometer senses 1 gravity when in its neutral

position, it must be capable of measuring this signal as well as heave. A 1.5 g instrument was chosen. Instruments are available for vertical measurement that use an internal spring to bias them to the neutral position. This would be of no benefit in this system, because the instrument would simply measure gravity in the opposite direction as the model rolled. Likewise, the sidle accelerometer, also affected by roll, was chosen to be 1.5 g. To allow some degree of standardization of components, the same sensing magnitude was chosen for the surge accelerometer.

It is felt that perhaps the specification of a maximum roll angle of 60° is excessive. If 45° were specified, the maximum variation in the gravity signal would be about 0.7 g. Since the maximum heave signal specified is approximately .31 g, a 1 g instrument could be used with very infrequent possibility of exceeding the rated accelerometer range. This would provide two important advantages over the selected instruments:

(a) the output sensitivity would be increased by about fifty percent, and

(b) the non-linearity and hysteresis error would be reduced by approximately the same percentage, since it is rated at 1% of full scale output and we are now reducing full scale output as well as restricting the signal to something less than before.

This improvement would be noticed most in the sidle accelerometer, for its desired signal is specified as only half that of the other two accelerometers.

B. Calibration and Error Analysis of the Linear Accelerometers

The calibration factors, as determined experimentally, are in

very close agreement with those furnished by the manufacturer. It should be noted that the calibration curves do not pass through the origin on Figures XVI and XVIII. This is due to the hysteresis of the instruments, and the discrepancy could probably be reduced by lowering the damping factors of these instruments and making it easier to zero the instruments when installing them in the model. However, if the instruments are installed as they now exist, proper zeroing procedures should reduce this discrepancy to negligible proportions.

The non-linearity and hysteresis errors are well within the manufacturer's specifications and should cause no trouble in data recording. On the surface, the errors appear to be greater than allowed by the system specifications, especially in the surge and sidle accelerometers. However, it must be remembered that in the actual model, a full excursion will not be experienced. The surge accelerometer will experience gravity due to pitching, but the maximum pitch is only 10°. This means the maximum gravity signal is only about one-half of gravity, thus restricting the non-linearity and hysteresis error to approximately one percent of full scale surge. The sidle accelerometer will experience about one gravity (due to roll and sidle) at its maximum signal. The error introduced here will be about $6\frac{1}{2}\%$ of the maximum sidle signal which means an accuracy within one-tenth of an inch for sidle displacement. It is anticipated that sixty degree rolls will be very rare and therefore, the error much reduced.

It is recommended that the excitation voltages be as high as possible (up to 9 volts maximum) in order to insure maximum accuracy and resolution (23). A large capacity battery source should be used to insure a constant level of voltage during model runs, and to

eliminate the presence of ripple ordinarily found in power supplies.

Figure XX is a plot showing the range of errors in acceleration due to linear accelerations normal to the sensitive axis. This range is defined as the area between curve A and any one of the other three curves and extends out to the line of maximum signal consistent with the signal assumed as A. For example, the maximum error in surge due to heave and sidle is .234 fps^2 or 1.87%. This chart provides a rapid means of determining the maximum error along any axis due to accelerations along the other two. The chart is based on the maximum sensitivity to transverse accelerations as specified by the manufacturer. It has been predicated by the thesis supervisor that this error is caused by misalignment between the sensing element and its case and can be eliminated (or reduced to a negligible quantity) by aligning the mass axis, rather than the case axis, with the model. This is done by rotating the accelerometer until its signal is nulled for all attitudes of the accelerometer when rotated about its sensitive axis. The accuracy of such a procedure, however, is limited by the hysteresis of the instrument. Since this particular error is an uncertainty error, it will be disregarded in the consideration of compensation systems for error signals.

The major error signal is that due to gravity. For example, the heave accelerometer senses a full gravity when vertical and may sense as little as a half g when rolled to 60 degrees. This is almost twice the signal it is desired to measure and therefore must be eliminated by a compensation system. Exact expression for the gravity error due to rotational motions have been developed in Appendix A for each of the three linear accelerometers.

$$\text{(Heave)} \qquad e = g \frac{\cos \phi \cos \psi}{(\cos^2 \phi + \cos^2 \psi - \cos^2 \phi \cos^2 \psi)^{\frac{1}{2}}} \qquad (1)$$

$$\text{(Surge)} \qquad e = g \frac{\sin \psi \cos \theta}{(\cos^2 \theta + \sin^2 \psi - \sin^2 \psi \cos^2 \theta)^{\frac{1}{2}}} \qquad (2)$$

$$\text{(Sidle)} \qquad e = g \frac{\sin \phi \cos \theta}{(\cos^2 \theta + \sin^2 \phi - \sin^2 \phi \cos^2 \theta)^{\frac{1}{2}}} \qquad (3)$$

The sensing system generates the three angles, so all that is left for the compensation system to do is to resolve these angles into usable form. Results of analysis of the heave error are shown in detail and a summary comparison is made for the other two linear motions.

Figures XXI and XXII show that the roll compensation system must include inputs from both roll and pitch to keep the error within acceptable limits.

A Taylor series approximation of the expression (Figure XXIII) showed that a fourth order equation would be required to keep the error within acceptable limits. Therefore, this method of analysis was abandoned in favor of a more direct type of trigonometric function generator.

Figure XXIV shows the results of attempts to simplify equation (1) by fairly simple approximations. The expression "$e = g \cos \phi \cos \psi$" shows great promise, since the error at simultaneous extreme roll and pitch is somewhat less than two percent.

Taylor series expansions for the surge and sidle expressions also required an equation of too high an order to be feasible (Appendix A).

Simplification in terms of trigonometric functions provided expressions somewhat easier to generate and the errors from these

approximations are considered negligible (Figures XXV and XXVI).

C. Proposed Gravity Error Compensation System

The proposed gravity compensation system is shown in Figure XXVII. Two systems were deemed possible for generating the trigonometric functions:

(a) servo driven sine-cosine potentiometers (21), (27)

(b) electronic sine-cosine operator (26).

Servo drives are used in most low frequency analogue computer work, since their response to low frequency signals is quite satisfactory. The sine-cosine operator is intended for use in high frequency repetitive systems. The high cost of such electronic units, along with the fact that either the sine or the cosine, but not both, is generated per unit, led to the selection of the servo system for generation of the gravity compensation signals.

No experimental work has been done with the proposed system, but a Gamewell (21) potentiometer was used in the laboratory simulation model (Figure XI) and some difficulty was experienced in nulling the gravitational signal. The sine-cosine operator was therefore mentioned above to call attention to it as a possible substitute should further experimentation prove the potentiometer unsatisfactory.

D. Proposed System

The complete system, exclusive of power supplies, is shown in block diagram form in Figure XXVIII. A mockup and partial analysis of the linear displacement system for one axis has been made and results (to be discussed later) look very promising.

The only equipment to be carried in the model is the package unit consisting of three linear accelerometers and three rate gyros. These components are to be placed in a small box known as the sensing unit.

The center of gravity and axes of the unit will be clearly marked on the unit case and should be placed exactly at the model center of gravity and the axes aligned with the model axes with extreme care. Failure to comply with this precaution will introduce serious errors into the linear acceleration sensing system. The accelerometers will be mounted as shown in Figure XIII.

The D.C. amplifiers (28) in the linear accelerometer circuits were originally included to bring the accelerometer outputs to satisfactory levels for use in the integrating amplifiers. However, they may prove to be unnecessary since the double integrating amplifier as it now exists (Figure V) has a gain built into it.

The double integrating amplifier is based on Philbrick USA-3 operational amplifiers (20)*. It works very well, once properly balanced, but balancing is a tedious process, and further refinement is necessary before the unit can be used effectively at the model basin. A basic refinement would be the replacement of the present balance potentiometer by a ten turn potentiometer with plus and minus voltages introduced from the two ends rather than with the switch presently installed. The magnitude of the balance voltage available should be increased to allow for balancing the amplifier over a greater range of unbalance.

E. Laboratory Data

The calibration curve for the sine-cosine potentiometer (21) is

---

* Supposedly, there are several good chopper stabilized D.C. operational amplifiers on the market, but no satisfactory ones are available at M.I.T. The Philbrick K3-J integrating amplifier (29), REAC integrating amplifier (30), and the DACL computer integrating amplifiers (no publications in existence) all have noise levels referred to the input that are in excess of those acceptable for this system.

quite erratic. Errors shown are a percent of the sine (or of gravity) and therefore would be higher when referred to specific model motions. The potentiometer used in the laboratory mockup is a rather old one and may therefore be worn. The fact that practically all errors are in the same direction may raise some doubt as to their validity, but in fact this is of little consequence, for it merely indicates poor zeroing. The erratic nature of the error is of most importance. The method of calibration is considered very accurate as are the precision potentiometer and galvanometer used. Since these errors are in excess of those guaranteed by the manufacturer, it is recommended that a new model be evaluated before any conclusions are drawn as to the feasibility of such a component.

The ability of the sine-cosine potentiometer to null the gravitational error of a linear accelerometer, as demonstrated in Figure XXX, shows promise. The error is consistent with that of the potentiometer calibration data and, as was stated previously, a new potentiometer should improve the results.

The integrator response, shown in Figure XXXII, is quite satisfactory since an output variation at the recorder of only ±2% is experienced over the entire anticipated operating range. The acceleration signal generated by the Scotch Yoke (Figure X) is itself subject to error because of play in its connection to the gear system. This could allow slapping at the peak displacements, thus giving an acceleration singularity and higher than actual displacement. This particular error will not appear in the actual system because the mounting will be rigid.

The frequency response curve shows that the double integrator is very good over the entire operating range. The slope is a constant

-20 dg per decade which shows the component is operating properly. The spread between the theoretical and experimental curves is merely a gain that was not predictable in theory and actually works to the advantage of the overall system. It is recommended that runs at an expanded time scale be made in order that phase differences between input and output may be measured. It should be remembered that the D.C. amplifier introduces a 180 degree phase shift, and therefore the output displacement's phase should correspond exactly to that of the input acceleration.

The expanded Sanborn recording at the beginning of the drift run (Figure XXXI) shows the system output in detail. It appears to be an undistorted sine wave, and therefore a close reproduction of the input displacement to the accelerometer. The noise superimposed on the acceleration chart is principally bearing noise from the Scotch Yoke and should be reproduced as a slight bumpiness in the displacement plot, for the motion is rough. A close examination of the plot will disclose this irregularity, thus attesting to the accuracy of the system. It should be reemphasized that this type of noise will not be present in the actual system.

The drift of the system is supposed to be negligible for the duration of a model run in the towing tank, a period of from two to three minutes. The ten minute drift run showed no drift over the normal run time and a very slight amount at the end of ten minutes. Since the double integrator is an imperfect integrator by intent, it should merely amplify and not integrate D.C. and very low frequency signals. Therefore, the recorded drift may be due to drift in the recording system and not in the integrator. This possibility should be investigated further by noting the drift of the recorder at zero

input, and then by noting the integrator drift at zero input.

A further test, suggested by the above discussion, is the response of the integrator to a step function. The gain of the integrators at zero frequency is approximately 100. Therefore, the output level should rise to 100 times the input level and then stop.

The Sanborn recording of the response of the system to a constant displacement at various frequencies shows a random noise in the displacement plot for 108 rpm. This is the same type of noise experienced in runs at a table inclination of 45 degrees. The natural frequency of the tilt table and its mounted equipment was found to be approximately 6 cycles per second. The noise frequency was .16 to .33 cps at 108 rpm and 0.1 to 0.2 cps at 76 rpm. An investigation should be made to determine whether this noise is due to mechanical or electrical sources.

V. CONCLUSIONS

1. The sensing elements selected are believed to be the optimum presently available components.
2. Space and weight limitations of model carried equipment are no longer a problem.
3. Model carried components must be positioned and aligned in the model with extreme accuracy or serious cross coupling errors will result.
4. The gravitational error due to rotation of the linear accelerometers into, and out of, the earth's gravitational field is the only error signal of the system large enough to require a special compensation system.
5. Servo driven sine-cosine potentiometers are presently considered the optimum method for generating gravity compensation signals. This is primarily due to their low cost, simplicity, and reliability. However, insufficient data has been obtained to fully evaluate their effectiveness.
6. The proposed system is capable of resolving the low level signals of the accelerometers and performing double integration over the entire anticipated frequency range with no noticeable attenuation of the output displacement signal.
7. The balancing system of the integrating amplifier, at the present stage of its development, is too critical for ease of operation and should be studied further.
8. The drift characteristic of the system is very satisfactory.
9. Large amplitude, low frequency, noise present during dynamic gravitational compensation studies must be eliminated before

further analysis of the linear displacement system can be made.

10. In view of the above, the proposed sensing system looks very promising. However, more analysis must be done before it can be properly evaluated.

VI. RECOMMENDATIONS

1. It is felt that the proposed system is adequate for motion measurements but that further studies should be made to refine the following components:

    a. The gravitational compensation system.

    b. The integrator balancing system.

2. Rate gyros should be procured and used as angular sensing elements in order to evaluate their performance while measuring angular motions as well as exciting the gravitational compensation system.

3. Further evaluation of the laboratory mockup should be made through the following tests:

    a. Expanding the time scale of the recorder to permit measurement of the phase difference between acceleration, velocity, and displacement. A phase lag is believed to exist since the amplifier operating range, positioned on the integrating slope of Figure XXXV , is too near the first break point of that curve.

    b. Graphical integration of the input signal for comparison with the output displacement, in conjunction with variation of the Scotch Yoke speed at a forty-five degree angle of tilt, to determine the nature of the interference signal superimposed on the displacement record.

    c. Observation of the response of the Double Integrating Summing Amplifier to a step function input.

VII. APPENDIX

APPENDIX A

DERIVATION SUMMARY

1. Expression for the Direct Axis Gravitational Errors:

   a. Heave Accelerometer

   From Figure XXXIV (a):

   $$e^2 + x^2 + y^2 = g^2$$

   where

   $$x = e \tan \psi$$

   and

   $$y = e \tan \phi$$

   Combining the above three expressions:

   $$e^2 + e^2 \tan^2 \psi + e^2 \tan^2 \phi = g^2$$

   $$e^2 (1 + \tan^2 \psi + \tan^2 \phi) = g^2$$

   $$e^2 (\sec^2 \psi + \sec^2 \phi - 1) = g^2$$

   $$e^2 \left(\frac{1}{\cos^2 \psi} + \frac{1}{\cos^2 \phi} - 1 \right) = g^2$$

   $$e^2 \left(\frac{\cos^2 \phi + \cos^2 \psi - \cos^2 \psi \cos^2 \phi}{\cos^2 \psi \cos^2 \phi} \right) = g^2$$

   Dividing through by the coefficient of e^2 and extracting the square root:

   $$e = g \frac{\cos \psi \cos \phi}{(\cos^2 \phi + \cos^2 \psi - \cos^2 \phi \cos^2 \psi)^{\frac{1}{2}}} \qquad (1)$$

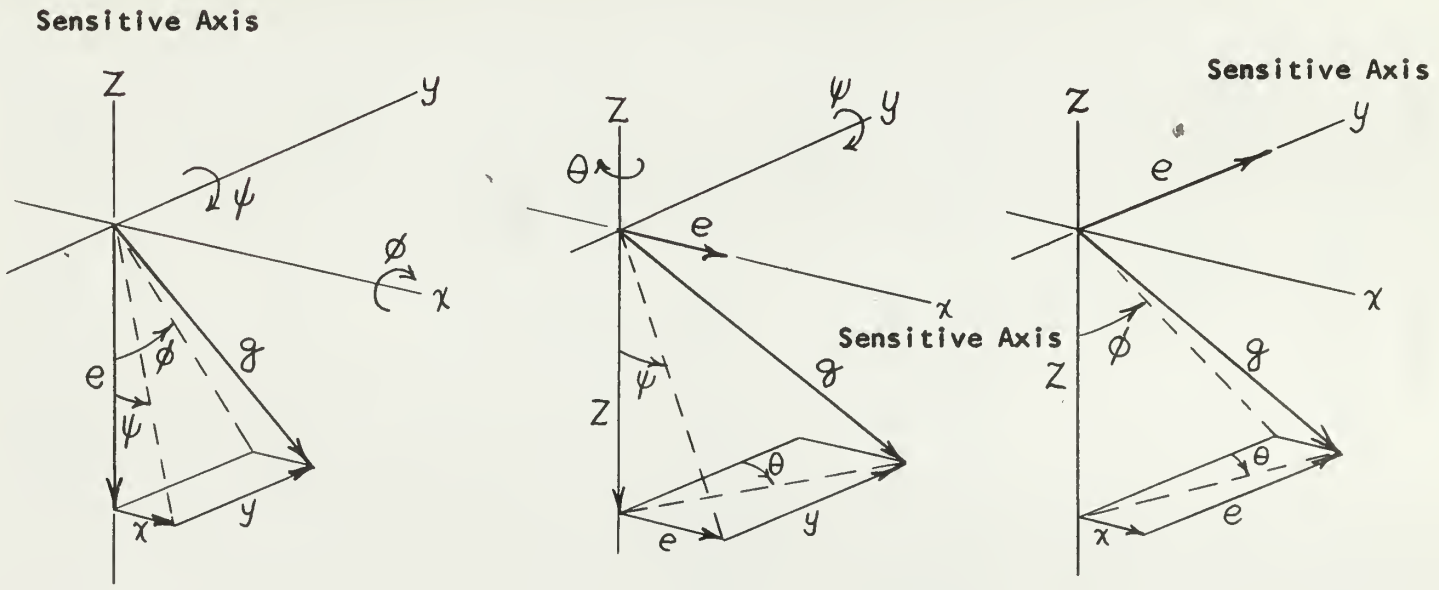

(a) Heave Accelerometer

(b) Surge Accelerometer

(c) Sidle Accelerometer

FIGURE XXXIV

Direct Axis Gravitational Errors Due to Angular Motion

b. Surge Accelerometer

From Figure XXXIV(b):

$$e^2 + y^2 + z^2 = g^2$$

where

$$y = e \tan \theta$$

and

$$z = e \cot \psi$$

Combining the above three expressions and simplifying in a manner similar to that for the heave accelerometer:

$$e = g \frac{\sin \psi \cos \theta}{(\cos^2\theta + \sin^2\psi - \sin^2\psi\cos^2\theta)^{\frac{1}{2}}} \qquad (2)$$

c. Sidle Accelerometer:

From Figure XXXIV (c):

$$e^2 + x^2 + z^2 = g^2$$

where

$$x = e \tan \theta$$

and

$$z = e \cot \phi$$

Comgining the above three expressions and simplifying in the same manner as in part b:

$$e = g \frac{\sin\phi \cos \theta}{(\cos^2\theta + \sin^2\phi - \sin^2\phi \cos^2\theta)^{\frac{1}{2}}} \qquad (3)$$

2. Taylor Series Expansion for the Heave Accelerometer Direct Axis Gravitational Error:

$$e = g \frac{\cos\psi \cos\phi}{(\cos^2\phi + \cos^2\psi - \cos^2\phi \cos^2\psi)^{\frac{1}{2}}} \qquad (1)$$

$$\cos\psi \cos\phi = \tfrac{1}{2}\left[\cos(\psi+\phi) + \cos(\psi-\phi)\right]$$

$$(\cos\psi\cos\phi)^2 = \tfrac{1}{4}\left[\cos^2(\psi+\phi) + \cos^2(\psi-\phi) + 2\cos(\psi+\phi)\cos(\psi-\phi)\right]$$

$$\cos^2\psi\cos^2\phi = \tfrac{1}{4}\left[\cos^2(\psi+\phi) + \cos^2(\psi-\phi) + \cos 2\psi + \cos 2\phi\right]$$

$$\cos^2\psi = \tfrac{1}{2}(1 + \cos 2\psi)$$

$$\cos^2\phi = \tfrac{1}{2}(1 + \cos 2\phi)$$

$$\cos^2(\psi+\phi) = \tfrac{1}{2}\left[1 + \cos 2(\psi+\phi)\right]$$

$$\cos^2(\psi-\phi) = \tfrac{1}{2}\left[1 + \cos 2(\psi-\phi)\right]$$

Substituting the above relations into equation (1):

$$e = g \frac{\frac{1}{2}\left[\cos(\psi+\phi) + \cos(\psi-\phi)\right]}{\left(\frac{1}{2}+\frac{1}{2}\cos 2\phi+\frac{1}{2}+\frac{1}{2}\cos 2\psi-\frac{1}{8}-\frac{1}{8}\cos 2(\psi+\phi)-\frac{1}{8}-\frac{1}{8}\cos 2(\psi-\phi)-\frac{1}{4}\cos 2\psi-\frac{1}{4}\cos 2\phi\right)^{1/2}}$$

$$e = g \frac{\frac{1}{2}\left[\cos(\psi+\phi)+\cos(\psi-\phi)\right]}{\left(\frac{3}{4}+\frac{1}{4}\left[\cos 2\phi+\cos 2\psi-\frac{1}{2}\cos 2(\psi-\phi)-\frac{1}{2}\cos 2(\psi+\phi)\right]\right)^{1/2}}$$

$$e = g \frac{\cos(\psi+\phi)+\cos(\psi-\phi)}{\left[3+\cos 2\phi+\cos 2\psi-\frac{1}{2}\cos 2(\psi-\phi)-\frac{1}{2}\cos 2(\psi+\phi)\right]^{1/2}} \qquad (1a)$$

Expanding Eq. (1a) into a Taylor Series:

$$\cos(\psi+\phi) = 1 - \frac{\psi^2+2\psi\phi+\phi^2}{2} + \frac{\psi^4+4\psi^3\phi+6\psi^2\phi^2+4\psi\phi^3+\phi^4}{24}$$

$$\frac{\psi^6+6\psi^5\phi+15\psi^4\phi^2+20\psi^3\phi^3+15\psi^2\phi^4+6\psi\phi^5+\phi^6}{720}$$

$$\cos(\psi-\phi) = 1 - \frac{\psi^2-2\psi\phi+\phi^2}{2} + \frac{\psi^4-4\psi^3\phi+6\psi^2\phi^2-4\psi\phi^3+\phi^4}{24}$$

$$- \frac{\psi^6-6\psi^5\phi+15\psi^4\phi^2-20\psi^3\phi^3+15\psi^2\phi^4-6\psi\phi^5+\phi^6}{720}$$

Summing the above gives an expression for the numerator of (1a):

$$\text{Num.} = 2 - \psi^2 - \phi^2 + \frac{\psi^4+\phi^4}{12} + \frac{\psi^2\phi^2}{2} - \frac{\psi^6+\phi^6}{360} - \frac{\psi^4\phi^2+\psi^2\phi^4}{24} + \cdots$$

Expanding the denominator terms of (1a):

$$\text{Cos}\,2\phi = 1 - 2\phi^2 + \frac{2}{3}\phi^4 - \frac{8}{90}\phi^6 + \cdots$$

$$\text{Cos}\,2\psi = 1 - 2\psi^2 + \frac{2}{3}\psi^4 - \frac{8}{90}\psi^6 + \cdots$$

$$-\tfrac{1}{2}\text{Cos}\,2(\psi-\phi) = -\tfrac{1}{2} + \psi^2 - 2\psi\phi + \phi^2 - \tfrac{1}{3}(\psi^4 - 4\psi^3\phi + 6\psi^2\phi^2 - 4\psi\phi^3 + \phi^4)$$
$$+\tfrac{2}{45}(\psi^6 - 6\psi^5\phi + 15\psi^4\phi^2 - 20\psi^3\phi^3 + 15\psi^2\phi^4 - 6\psi\phi^5 + \phi^6) + \cdots$$

$$-\tfrac{1}{2}\text{Cos}\,2(\psi+\phi) = -\tfrac{1}{2} + \psi^2 + 2\psi\phi + \phi^2 - \tfrac{1}{3}(\psi^4 + 4\psi^3\phi + 6\psi^2\phi^2 + 4\psi\phi^3 + \phi^4)$$
$$+\tfrac{2}{45}(\psi^6 + 6\psi^5\phi + 15\psi^4\phi^2 + 20\psi^3\phi^3 + 15\psi^2\phi^4 + 6\psi\phi^5 + \phi^6) + \cdots$$

Combining terms the denominator becomes:

$$\text{Denom.} = (4 - 4\psi^2\phi^2 + \tfrac{4}{3}[\psi^4\phi^2 + \psi^2\phi^4] + \cdots)^{\frac{1}{2}}$$

The series expression for (1) Ls, therefore:

$$e = g\,\frac{2 - (\psi^2+\phi^2) + \frac{1}{2}\psi^2\phi^2 + \frac{1}{12}(\psi^4+\phi^4) - \frac{1}{24}(\psi^4\phi^2+\psi^2\phi^4 - \frac{1}{360}(\psi^6+\phi^6) + \cdots}{(4 - 4\psi^2\phi^2 + \frac{4}{3}[\psi^4\phi^2+\psi^2\phi^4] + \cdots)^{\frac{1}{2}}} \qquad (1b)$$

3. Derivation of the Operational Amplifier Feedback Loop

A schematic diagram of an electronic integrator is shown in Figure XXXV. A perfect integrator would not have R_f across C. R_f was placed there to prevent the integration of D.C. and low frequency signals, thus reducing drift. It is hoped that the low gain at high frequencies will prevent interference from high frequency noise.

$$\frac{e_o}{e_g} = -A \quad \text{or} \quad e_g = -\frac{1}{A} e_o \tag{4}$$

$$e_i - e_g = iR_i \tag{5}$$

$$e_g - e_o = -e_o\left(\frac{1}{A} + 1\right) = iZ_f$$

where

$$Z_f = \frac{R_f}{1 + j\omega CR_f}$$

$$1 \gg \frac{1}{A} = 10^{-8}$$

Therefore

$$-e_o = \frac{iR_f}{1 + j\omega CR_f} \quad \text{or}$$

$$i = \frac{-e_o(1 + j\omega CR_f)}{R_f} \tag{6}$$

Substituting Eq. (4) and (6) into (5)

$$e_i + \frac{e_o}{A} = -e_o \frac{R_i}{R_f}(1 + j\omega CR_f)$$

($\frac{e_o}{A} \to 0$)

Therefore

$$\frac{e_o}{e_i} = -\frac{R_f}{R_1} \cdot \frac{1}{1 + j\omega CR_f} \tag{7}$$

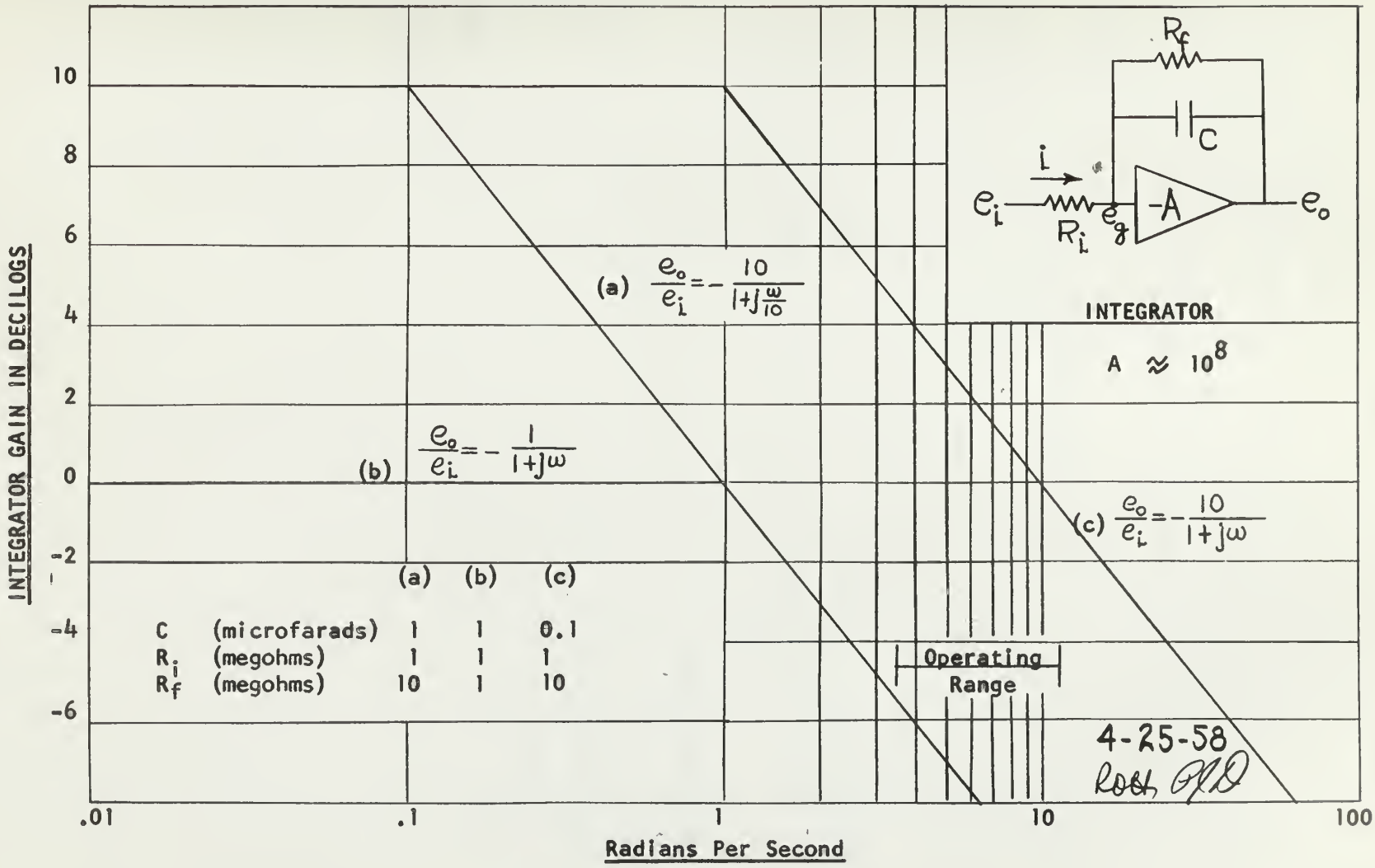

FIGURE XXXV

Theoretical Frequency Response of a Single Integrator

Plot (a) of Figure XXXV makes use of a real time integrator (R_iC = 1 sec) modified by R_f. The frequency to be used in the mockup (Figure X) is approximately 8 radians per second (76 RPM). At this frequency the gain is -9.15 dg or 0.122. This is not very satisfactory for a gain of at least unity (for recording purposes) should be attempted.

It can be seen from Figure XXXV that if the plot were to cross the 0 dg. line at a frequency of 10 radians per second, the time constant (CR_f) would have to be 1 second for a steady state gain of 10.

If C were to remain 1.0 microfarad , R_f would have to be reduced to one megohm. It is desired to keep R_i at least one megohm. Therefore, the steady state gain would be reduced to 1 (0 dg). This is illustrated in plot b. This would gain nothing.

However, if the capacitance is varied, the steady state gain remains constant, and only the break point varies. Let the steady state gain be 10 (R_f = 10 R_i = 10 megohms). To have gains greater than unity over the operating range, let C be 0.1 microfarads. The gain at calibration frequency will then be +1 dg or 1.25. This is satisfactory. (See plot (c)).

APPENDIX B

Summary of Data and Calculations

TABLE III

Calibration of Accelerometer No. 6429

Column #1	#2	#3	#4	Column #1	#2	#3	#4
0	32.165	17.0	3.64	180	-32.165	-16.80	- .19
10	31.676	16.7	2.87	190	-31.676	-16.54	- .19
20	30.225	15.93	2.49	200	-30.225	-15.755	-1.05
30	27.855	14.671	2.16	210	-27.555	-14.498	-1.15
40	24.638	12.959	1.57	220	-24.638	-12.802	-1.44
50	20.676	10.854	0.94	230	-20.676	-10.736	-1.32
60	16.083	8.394	-0.21	240	-16.083	- 8.326	-1.51
70	11.000	5.715	-0.65	250	-11.000	- 5.670	-1.51
80	5.584	2.868	-0.98	260	- 5.584	- 2.842	-1.47
90	0.000	- .0525	∓1.00	270	0.000	+ 0.066	∓1.26
100	- 5.584	- 2.978	1.13	280	5.584	2.985	1.26
110	-11.000	- 5.825	1.45	290	11.000	5.808	1.13
120	-16.083	- 8.480	1.44	300	16.083	8.457	1.00
130	-20.676	-10.880	1.44	310	20.676	10.847	0.80
140	-24.638	-12.938	1.16	320	24.638	12.899	0.42
150	-27.855	-14.612	1.01	330	27.855	14.565	0.13
160	-30.225	-15.831	.57	340	30.225	15.781	-0.36
170	-31.676	-16.58	- .57	350	31.676	16.51	-0.77
				360	32.165	16.75	-1.15

Column #1: Angle of Rotation

Column #2: Acceleration in fps^2

Column #3: Output in Millivolts

Column #4: Non-linearity and hysteresis error as a % of z(max)

TABLE IV

Calibration of Accelerometer No. 3023

Column #1	#2	#3	#4	Column #1	#2	#3	#4
0	0.000	0.080	-8.27	180	0.000	0.535	± 6.37
10	5.584	2.750	-8.62	190	- 5.584	- 2.159	- 5.95
20	11.000	5.338	-8.97	200	-11.000	- 4.779	- 5.28
30	16.083	7.801	-8.20	210	-16.083	- 7.235	- 4.73
40	20.676	10.033	-7.30	220	-20.676	- 9.463	- 3.96
50	24.638	11.974	-6.09	230	-24.638	-11.389	- 3.22
60	27.855	13.560	-4.73	240	-27.855	-12.957	- 2.44
70	30.225	14.741	-3.41	250	-30.225	-14.112	- 1.86
80	31.676	15.489	-1.64	260	-31.676	-14.848	- 0.58
90	32.165	15.775	0	270	-32.165	-15.102	0.32
100	31.676	15.585	1.45	280	-31.676	-14.902	1.16
110	30.225	14.941	3.92	290	-30.225	-14.239	2.22
120	27.855	13.840	4.28	300	-27.855	-13.141	3.48
130	24.638	12.337	5.60	310	-24.638	-11.643	4.96
140	20.676	10.462	6.50	320	-20.676	- 9.796	6.75
150	16.083	8.276	7.08	330	-16.083	- 7.633	8.08
160	11.000	5.819	6.50	340	-11.000	- 5.239	9.53
170	5.584	3.226	6.70	350	- 5.584	- 2.668	10.41
				360	0.000	- 0.004	±10.96

Column #1: Angle of Rotation

Column #2: Acceleration in fps^2

Column #3: Output in millivolts

Column #4: Non-linearity and hysteresis error as a % of y(max)

TABLE V

Calibration of Accelerometer No. 3024

Column #1	#2	#3	#4	Column #1	#2	#3	#4
0	0.000	- 0.041	-6.79	180	0.000	0.703	± 4.69
10	5.584	2.735	-6.85	190	- 5.584	- 2.091	- 4.47
20	11.000	5.441	-6.70	200	-11.000	- 4.824	- 3.90
30	16.083	8.015	-6.02	210	-16.083	- 7.371	- 3.64
40	20.676	10.346	-5.32	220	-20.676	- 9.696	- 3.04
50	24.638	12.389	-4.25	230	-24.638	-11.696	- 2.62
60	27.855	14.045	-3.40	240	-27.855	-13.330	- 2.11
70	30.225	15.290	-2.38	250	-30.225	-14.547	- 1.53
80	31.676	16.074	-1.43	260	-31.676	-15.309	- 0.92
90	32.165	16.41	0	270	-32.165	-15.612	0.
100	31.676	16.24	1.12	280	-31.676	-15.427	0.89
110	30.225	15.578	2.06	290	-30.225	-14.782	2.10
120	27.855	14.470	3.16	300	-27.855	-13.689	3.42
130	24.638	12.941	4.27	310	-24.638	-12.177	4.80
140	20.676	11.013	4.96	320	-20.676	-10.285	6.05
150	16.083	8.751	5.34	330	-16.083	- 8.071	7.15
160	11.000	6.211	5.19	340	-11.000	- 5.595	7.99
170	5.584	3.518	5.23	350	- 5.584	- 2.985	9.30
				360	0.000	- 0.164	10.21

Column #1: Angle of Rotation

Column #2: Acceleration in fps^2

Column #3: Output in Millivolts

Column #4: Non-linearity and hysteresis error as a % of x(max)

TABLE VI

Evaluation of Exact Expression for Gravitational Error in the Heave Accelerometer at Various Angles of Roll for Fixed Angles of Pitch

ϕ°	$(e/g)_{exact}$; Eq. (1)		
	$\psi = 0^\circ$	$\psi = 5^\circ$	$\psi = 10^\circ$
0	1.000	.9962	.9848
10	.9848	.9812	.9703
20	.9397	.9366	.9270
30	.8660	.8636	.8559
40	.7660	.7643	.7589
50	.6428	.6418	.6387
60	.5000	.4995	.4981

TABLE VII

Percent Difference Between Gravitational Signal of the Heave Accelerometer for Various Pitch Angles Expressed as a Percent of the Maximum Predicted Heave Signal (10 fps^2)

ϕ°	*% Diff. between columns of constant ψ		
	$0^\circ - 5^\circ$	$0^\circ - 10^\circ$	$5^\circ - 10^\circ$
0	1.22	4.89	3.61
10	1.16	4.67	3.51
20	1.00	4.09	3.09
30	.77	3.25	2.48
40	.55	2.29	1.74
50	.32	1.32	1.00
60	.16	.61	.45

* % Difference is referred to the maximum heave signal

TABLE VIII

Percent Error due to Series Approximations of Gravitational Error in the Heave Accelerometer for Various Roll Angles at Constant Pitch Angles of Zero and Ten Degrees

	Δe in percent of maximum heave signal					
ϕ°	$\psi = 0$			$\psi = 10^\circ$		
	Eq. (1b)	Eq. (1b)*	Eq. (1b)**	Eq. (1b)	Eq. (1b)*	Eq. (1b)**
0	0	0	0	0	0	0
5	0	0	0	.0322	0	.2576
10	0	0	0	.0966	0	.2576
15	0	0	.0322	0	- .0644	.5474
20	0	.0322	.1932	.0322	.0966	1.030
25	0	0	.483	.1610	0	1.835
30	0	0	.9982	-.0644	.0644	2.673
35	0	0	1.868	-.0966	- .4508	3.928
40	0	.0644	3.091	-.0322	- .3542	5.732
45	0	.0966	4.991	+.0322	- .4830	8.179
50	0	.1932	7.599	.1288	- .8372	11.21
55	0	.3542	11.045	.2254	-1.288	14.97
60	0	.5796	15.553	.3542	-1.739	19.83

* Eq. (1b) through fourth order terms. Appendix A.

** Eq. (1b) through second order terms. Appendix A.

TABLE IX

Analysis of Gravitational Error in Sidle and Surge Accelerometers

ϕ	#1	#2	#3	ψ	#4	#5
5	.0872	.0871	- .0537	5	.0871	-.0250
10	.1737	.1736	- .0537	10	.1736	-.0250
15	.2588	.2587	- .0537	15	.2587	-.0250
20	.3420	.3419	- .0537			
25	.4226	.4223	- .1610			
30	.5000	.4995	- .2684			
35	.5736	.5728	- .4294			
40	.6428	.6418	- .5367			
45	.7071	.7057	- .7514			
50	.7660	.7642	- .9660			
55	.8192	.8171	-1.127			
60	.8660	.8635	-1.342			

Column #1 and #2 are Eq. (3) Appendix A divided by "g" evaluated at $\theta = 0^{\circ}$ and 5° respectively.

Column #3 is the percent difference between columns #1 and #2 referred to a maximum sidle signal of 6 fps^2.

Column #1 and #4 are Eq. (2) Appendix A divided by "g" evaluated at $\theta = 0^{\circ}$ and 5° respectively.

Column #5 is the percent difference between columns #1 and #4 referred to a maximum surge signal of 12.5 fps^2.

TABLE X

Calibration of Gamewell RL-14MS Sine-Cosine Potentiometer

Column #1	#2	#3	Column #1	#2	#3
1	91.65	.63	19	271.65	- .04
2	101.65	.38	20	281.65	.62
3	111.65	- .11	21	291.65	.99
4	121.65	.98	22	301.65	.79
5	131.65	.69	23	311.65	.02
6	141.65	.77	24	321.65	.16
7	151.65	1.11	25	331.65	.03
8	161.65	1.26	26	341.65	.44
9	171.65	1.99	27	351.65	.10
10	181.65	.16	28	1.65	1.14
11	191.65	- .77	29	11.65	.61
12	201.65	1.10	30	21.65	.67
13	211.65	.64	31	31.65	- .52
14	221.65	1.35	32	41.65	.30
15	231.65	.55	33	51.65	- .06
16	241.65	.72	34	61.65	.08
17	251.65	.04	35	71.65	.04
18	261.65	- .69	36	81.65	- .58

Column #1: Rotational Position

Column #2: Pot. Setting in Degrees

Column #3: Error as a % of maximum signal

TABLE XI

Ability of Sine-Cosine Potentiometer to Null Gravitational Errors

Column #1	#2	#3	#4	#5
45°	15.236	15.236	0	0
40	13.890	13.850	.04	.186
35	12.480	12.360	.12	.557
30	10.813	10.664	.149	.691
25	9.205	8.964	.241	1.12
20	7.480	7.250	.230	1.07
15	5.655	5.416	.239	1.11
10	3.735	3.430	.305	1.42
5	1.908	1.606	.302	1.40
0	0.000	- .020	.02	.093

Column #1: Inclination of Accelerometer from Horizontal

Column #2: Accelerometer Output (mv)

Column #3: Potentiometer Output (mv)

Column #4: Column #2 minus #3

Column #5: Percent Error Referred to "g"

TABLE XII

Frequency Response of Double Integrating Amplifier

RPM	108	76	56	33	15
Rad/sec	11.3	7.98	5.86	3.46	1.57
Cycles/sec.	1.80	1.27	.933	.55	.25
Acc. Input (mv)*	16.65	8.39	4.53	1.58	.325
Output (mv)	2950	3000	2950	2800	2125
$G = \frac{\text{output}}{A \cdot \text{input}}$	1.772	3.58	6.51	17.72	65.5
$dg = 10 \log = \lvert G \rvert$	2.50	5.54	8.04	12.50	18.17

F = Calibration Factor (Accelerometer No. 3024): 2.571 mv/volt·g

* $\therefore$ acceleration input = $V_b \times \frac{F \times a}{g}$

$$\text{where } a = \frac{s \times 4\pi^2}{T^2} = \frac{\frac{2.337}{12} \times 4\pi^2 (RPM)^2}{3600}$$

$$a = .0213\ (RPM)^2$$

A = Video amplifier gain = 100

V_b = Accelerometer excitation voltage = 8.04 volts (DC)

APPENDIX C

Sample Calculations

1. Calculation of Tangential Accelerations Due to Roll, Pitch, and Yaw

$$a_t = \frac{\text{(axial separation of transducers-inches)}}{12} \times \alpha$$

$$a_{t_\phi} = \frac{(4 \text{ in.})}{12} (2.88 \text{ rad/sec}^2) = .96 \text{ fps}^2$$

$$a_{t_\psi} = \frac{(8 \text{ in.})}{12} (1.92 \text{ rad/sec}^2) = 1.28 \text{ fps}^2$$

$$a_{t_\theta} = \frac{(8 \text{ in.})}{12} (.54 \text{ rad/sec}^2) = .36 \text{ fps}^2$$

2. Calculation of Linear Accelerometer Errors Due to Rotational Motions of the Model.*

y = r x = z = 0	x = r y = z = 0	z = r x = y = 0
$a_{y_\phi} = \frac{r(\text{inches})}{12}\omega_\phi^2 = 2.52\ r$	$a_{x_\psi} = \frac{r}{12}\omega_\psi^2 = .279\ r$	$a_{z_\phi} = \frac{r}{12}\omega_\phi^2 = 2.52\ r$
$a_{y_\theta} = \frac{r}{12}\omega_\theta^2 = .0392\ r$	$a_{x_\theta} = \frac{r}{12}\omega_\theta^2 = .0392$	$a_{z_\psi} = \frac{r}{12}\omega_\psi^2 = .279\ r$
$a_y = a_{y_\phi} + a_{y_\theta}$	$a_x = a_{x_\psi} + a_{x_\theta}$	$a_z = a_{z_\phi} + a_{z_\psi}$
$a_{z_\phi} = \frac{r}{12}\alpha_\phi = .24\ r$	$a_{z_\psi} = \frac{r}{12}\alpha_\psi = .16\ r$	$a_{z_\phi} = \frac{r}{12}\alpha_\phi = .24\ r$
$a_{x_\theta} = \frac{r}{12}\alpha_\theta = .045\ r$	$a_{y_\theta} = \frac{r}{12}\alpha_\theta = .045\ r$	$a_{x_\psi} = \frac{r}{12}\alpha_\psi = .16\ r$

* See Figure XXXVI

FIGURE XXXVI

Linear Accelerations Induced by Angular Motion

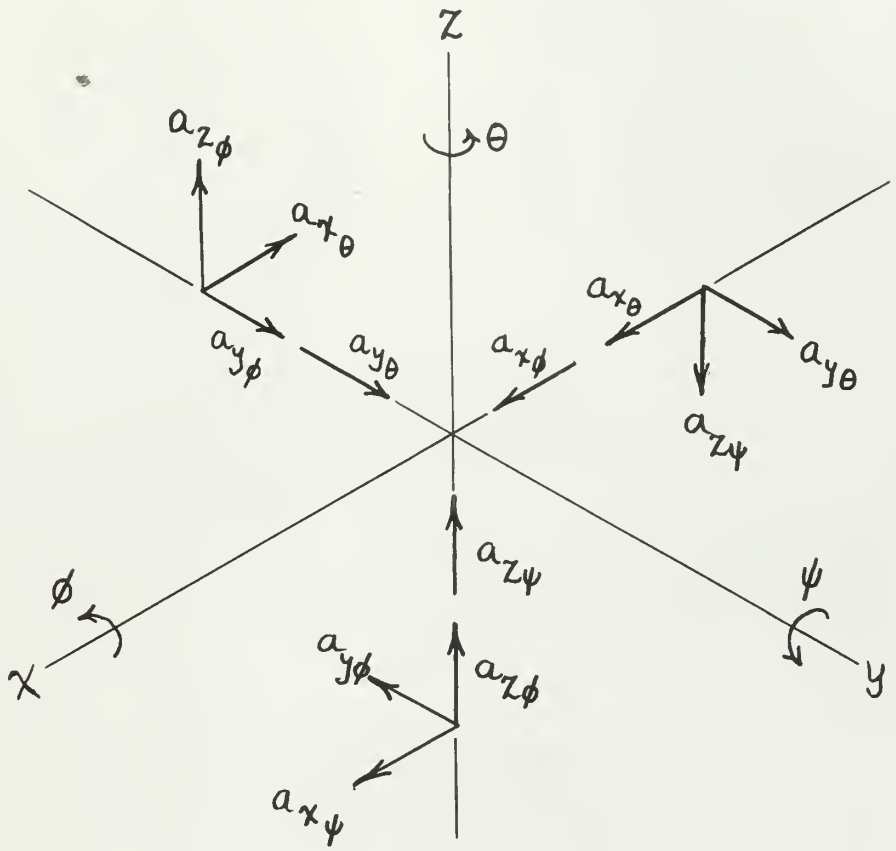

Normal Accelerations

$a_x = - X \omega_\psi^2$

$a_z = - Z \omega_\psi^2$

$a_{z\phi} = - Z \omega^2{}_\phi$

$a_{y\phi} = - Y \omega^2{}_\phi$

$a_{y\theta} = - Y \omega^2{}_\theta$

$a_{x\theta} = - X \omega^2{}_\theta$

Tangential Accelerations

$a_x = - X \alpha_\psi$

$a_z = - Z \alpha_\psi$

$a_{z\phi} = - Z \alpha_\phi$

$a_{y\phi} = - Y \alpha_\phi$

$a_{y\theta} = - Y \alpha_\theta$

$a_{x\theta} = - X \alpha_\theta$

3. Calculation of Resistance Values to be Used in Sine-Cosine Potentiometer Voltage Divider Network

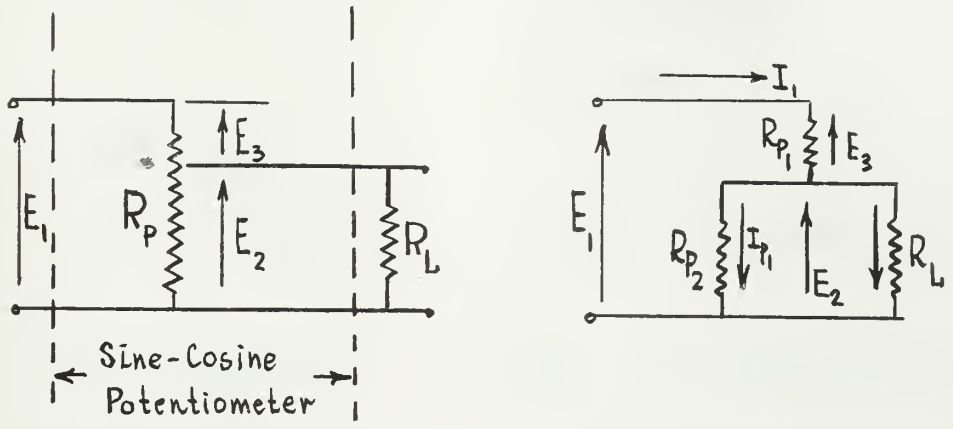

1) E_1 varies sinusoidally from $0 \rightarrow |E_1|$

2) Consider adding R_L

$$E_2 = E_1 - E_3 \qquad I_1 = \frac{E_1}{R_{p_1} + \dfrac{R_{p_2} R_L}{R_{p_2} + R_L}}$$

$$E_2 = E_1 - \frac{E_1 R_{p_1}(R_{p_2} + R_L)}{R_{p_1}(R_{p_2} + R_L) + R_{p_2} R_L}$$

$$= E_1 \left[\frac{R_{p_2} R_L}{R_{p_1} R_{p_2} + R_{p_1} R_L + R_{p_2} R_L} \right]$$

Let $R_L \gg R_{p_2}$; $R_L \gg R_{p_1}$

$$\therefore E_2 = E_1 \left[\frac{R_{p_2}}{R_{p_1} + R_{p_2}} \right]$$

4. Calculation of Motor Speed to Obtain a Given Acceleration, at a Particular Displacement Amplitude

$$s = |s| \sin \omega t \qquad |s| = \frac{4.763 \text{ (Double Amplitude) inches}}{2 \times 12}$$

$$\omega = \frac{2\pi}{T} \text{ rad/sec}$$

Differentiating

$$a = \frac{-4.763}{24} \times \frac{4\pi^2}{T^2} \sin \omega t \qquad \text{Let } |a| = 12.5 \text{ fps}^2$$

$$\therefore T^2 = \frac{-4.763\ (4\pi^2)}{24\ a} \qquad T^2 = .628 \qquad T = .792 \text{ sec/cycle}$$

$$f = \frac{1}{.792} = 1.262 \text{ cps}$$

RPM = 60 (1.262) = 76

5. Calculation of Signal Attenuation Upon Integration

Consider $a = A \sin \omega t$ A is acceleration amplitude.

$$v = -\frac{A}{\omega} \cos \omega t$$

$$s = -\frac{A}{\omega^2} \sin \omega t \quad \text{or} \quad s = -A\left[\frac{T^2}{4\pi^2}\right] \sin \omega t$$

If $\frac{T}{2\pi} < 1$: Signal voltage will be attenuated upon integration

If $\frac{T}{2\pi} > 1$: Signal voltage will be amplified upon integration

Therefore, in order for the signal to be amplified, the period must be greater than 6.28 sec. Since the predicted periods are approximately one second, the integrating circuits must have an amplification of at least 6.28 to prevent signal attenuation.

APPENDIX D

Equipment Used in Various Tests

1. Static Calibration of the Linear Accelerometers

   (a) Hardinge Milling Machine Dividing Head, Serial #705. Hardinge Brothers, Inc., Elmira, N. Y.

   (b) Four jaw lathe chuck, five-inch, Mo. 9405-S, Serial #44. Union Mfg. Co., New Britain, Conn.

   (c) Rubicon Precision Potentiometer, Serial #42765.

   (d) Rubicon Galvanometer (external) for use with item (c), Serial #E-062.

   (e) Vacuum Tube Voltmeter, Simpson Electric Company, Chicago, Model 303.

   (f) One Burgess F4BP 6.0 volt battery.

2. Static Calibration of the Sine-Cosine Potentiometer

   (a) Items (a) through (f) of paragraph number 1.

   (b) Sine-Cosine Potentiometer, Gamewell RL-14MS, Serial #674, Terminals B-D, Card Resistance 35,400 ohms.

   (c) Two "Ohmite" resistors, 3.6 meg-ohm, and 10,000 ohms respectively.

3. Ability of the Sine-Cosine Potentiometer to Null Gravitational Errors

   (a) Items (c), (d), and (e) of paragraph 1.

   (b) The calibrating table shown in Figure IV.

   (c) Statham A6a-1.5-350 linear accelerometer Serial #3023.

   (d) One Burgess 4FH 1.5 volt battery. Potentiometer excitation.

   (e) One Burgess 5540 7.5 volt "c" battery. Potentiometer excitation.

   (f) Decade Resistance Type 602-J, Serial #5041, General Radio, Cambridge, Mass.

(g) One 3.6 meg-ohm "Ohmite" carbon resistor.

(h) Item (b) of paragraph 2.

(i) One Willard DD-3-3, 6 volt, three cell, automobile type battery. Accelerometer excitation.

(j) One Willard DD-7-1, 2 volt, single wet cell, battery. Accelerometer excitation.

4. Double Integrator Response to a Constant Displacement Input

(a) Philbrick Power Supply with Sorensen Regulated A.C. Power Supply. Sorensen & Co., Inc., Serial 2-664, Model 2000-S.

(b) The Double Integrating Summing Amplifier shown pictorially in Figure III, and schematically in Figure V.

(c) Twin-Viso Recorder, Sanborn Company, Cambridge, Mass. Model 60-1300, Serial #24. D.C. Pre-Amplifier Model 60-400, Serial #114. D.C. Amplifier channel "A" Model 64-300A, Serial #393, channel "B" Model 64-300A Serial #376.

(d) D.C. Amplifier, Video Instruments Co., Inc. 2340 Sawtelle Blvd., Los Angeles 64, California. Model 71, Serial 129.

(e) Scotch Yoke Drive, see Figure X.

Motor Data:

Electro Machines Inc., Cedarburg, Wisconsin.

A.C. Motor	Volts 220
Type P	Amps 4
Frame D42S	60 cps
H.P. 1.0	3 phase
RPM 3450	Rating 40°C

Variable Speed Transmission

Graham Transmission Inc., Milwaukee, Wisconsin.

Model 225
Serial #73039
Output RPM 1200
Input RPM 3600

(f) Items (b), (c), (i), and (j) of paragraph 3.

(g) Item (e) of paragraph 1.

5. Dynamic Gravitational Error Compensation of the Linear Accelerometer Signal at Fixed Angles of Inclination

(a) All of the equipment listed under paragraph 4.

(b) Item (b) of paragraph 2.

(c) Items (d) and (e) of paragraph 3.

(d) Decade Resistor 11.1-k ohm, General Radio.

APPENDIX E

LITERATURE CITATIONS

1. Draper, C. S., McKay, W., and Lees, S., "Instrument Engineering" McGraw-Hill Book Co., Inc., New York, 1955.

2. Lewis, E. V., "Ship Speeds in Irregular Seas", Trans. SNAME*, vol. 63, 1955.

3. "Specifications for Linear Accelerometers", Bulletin A-1(1), March 1957, Statham Laboratories Inc., 12401 W. Olympic Blvd., Los Angeles, California.

4. Williams, S. B., and Atchley, R. D., "A Precision Accelerometer", M.I.T. Dynamic Analysis and Control Laboratory, Meteor Report #35, February 1949.

5. Allnutt, R. B., and Mintz, F., "Instruments at the David Taylor Model Basin for Measuring Vibration and Shock on Ship Structures and Machinery", DTMB Report 563, U.S. Navy, July 1948.

6. Draper, C. S., Wrigley, W., and Grohe, L. R., "The Floating Gyro and its Application to Geometrical Stabilization Problems on Moving Bases." IAS Preprint No. 503, January 1955.

7. Porter, W. R., "Angular Motion Instrumentation for Model Seaworthiness Testing", M.I.T. Servomechanisms Laboratory. Technical Memorandum 6897-TM-19, Contract NOrd 11799. May 23, 1955.

8. "Subminiature Precision Rate Gyroscopes", Technical Data Handbook SA78A-4. U.S. Time Corp., 500 Fifth Avenue, New York.

9. "U.S. Time Rate Gyroscope", Brochure No. SA78-4. U.S.T. Corp., 500 Fifth Avenue, New York.

10. "Miniature Rate Gyroscope, Model GN Golden Gnat", Bulletin GN 1M 2-58, Minneapolis-Honeywell, Boston Division, 1400 Soldiers Field Road, Boston 35, Mass.

11. "Specifications for Unbonded Strain Gage Liquid Rotor Angular Accelerometers", Bulletin No. AA1(1), Statham Laboratories, Inc., November 1956.

12. White, G., "Response Characteristics of a Simple Instrument", Statham Instrument Notes, No. 2, Statham Laboratories, Inc., April-May 1948.

---

* Society of Naval Architects and Marine Engineers

13. Levy, S. and Kroll, W. D., "Response of Accelerometers to Transient Accelerations", Journal of Research of the National Bureau of Standards, Vol. 45, No. 4, October 1950, Research Paper 2138.

14. "Statham Transducer Element", Bulletin No. 1.0, Statham Laboratories, Inc., March 1957.

15. "Calibrating Resistors", Bulletin No. 600, Statham Laboratories, Inc., May 1957.

16. White, G., "Calibration and Test of Accelerometers", Instrument Note No. 6, Statham Laboratories, Inc., October 1957.

17. Grant, E., "A Note on Regulated Power Supplies", Instrument Note No. 18, Statham Laboratories, Inc., November-December 1950.

18. White, G., "Secondary Effects in Seismic System Instruments", ASME, National Applied Mechanics Conference, Pennsylvania State College, June 1952.

19. Orlacchio, A. W., and Hieber, G., "Trends in Acceleration Measurement", Proceedings of the Second IRE Conference, Atlanta, Georgia, December 1956.

20. "Universal Stabilized Amplifier", GAP/R Technical Bulletin USA-3, George A. Philbrick Researches, Inc., Boston, Mass.

21. "Precision Potentiometers" Catalog, The Gamewell Company, Newton Upper Falls 64, Mass.

22. Draper, C. S., and Lees, S., "Instrumentation Problems of Inertial Guidance", For Presentation at the Conference on Instrumentation, Gordan Research Conference, New London, New Hampshire, July 1957.

23. Li, Y. T., "Dynamic Measurements", Department of Aeronautical Engineering, M.I.T.

24. Hagen, G. R., "Feasibility Studies of the Roll Stabilization of the USS Boston (CAG-1)", DTMB Report 950, September 1955.

25. Weinblum, G., and St. Denis, M., "On the Motions of Ships at Sea", Trans. SNAME, vol. 58, 1950.

26. Pinckney, R. P., and Giser, S., "The Sine-Cosine Operator", M.I.T. Instrumentation Laboratory Report R-73, April 1954.

27. "RVP3-S59-3 Sine-Cosine Precision Potentiometer", Bulletin P-142, Technology Instrument Corporation, Acton, Mass., 30 May 1956.

28. "Operating Instructions for Model 71 D.C. Amplifier", Video Instruments, Inc., Los Angeles, California.

29. "Model K3-J Integrating Component", Electronic Analog Computing Instruments, George A. Philbrick Researches, Inc., Boston, Mass.

30. "Theory and Operation Manual — E. E. Department REAC Analog Computer", M.I.T. Servomechanisms Laboratory Report No. 6080-1, 15 March 1954.

31. "Servo Systems and Data Transmission", TM 11-674, Department of The Army Technical Manual, August 1952.

32. Blackburn, J. F., "Components Handbook", M.I.T. Radiation Laboratory Series, vol. 17, McGraw-Hill Book Co., Inc., New York, 1949.

33. "Instructions for Operation and Maintenance of Twin-Viso Cardiette-Model 60", Sanborn Company, Cambridge, Mass.

34. Manning, G. C., "Theoretical Naval Architecture", Chap. 8, Department of Naval Architecture and Marine Engineering, M.I.T.

35. Abkowitz, M. A., "Correlation of Model Tests in Waves--Report of Panel", American Towing Tank Conference, September 1956.

36. Van Lammeren, W. P. A., and Vossers, G., "The Seakeeping Laboratory of the Netherlands Ship Model Basin", International Shipbuilding Progress, Volume 4, No. 29, January 1957, pg. 3.

37. Abkowitz, M. A., and Paulling, J. R., Jr., "The Ship Model Towing Tank at M.I.T." Trans. SNAME, vol. 61, 1953.

38. "Operating Directions - Rubicon Portable Precision Potentiometer, Catalog No. 2702", Rubicon Company, Philadelphia, Pa.

39. Paulling, J. R., Jr., "Towing and Motion Measurement Instrumentation for Model Seakeeping Investigations", University of California Institute of Engineering Research, Berkeley, California, June 1956.

40. Adams, H. C., "Some Notes on the Use of Models in the Study of the Rolling of Ships", Trans. SNAME, 1938.

41. Paulling, J. R., Jr., "Model Seaworthiness Testing Technique and the Effect of Anti-Pitching Fins", S. M. Thesis, M.I.T. 1953.

42. Kerwin and Stange, "A Method of Determining the Motion of a Ship Model in Waves", B.S. Thesis, M.I.T. 1953.

43. St. Denis, M., and Pierson, W. J., "On the Motions of Ships in Confused Seas", Trans. SNAME, 1953.